



OPEN Grouting uplift for structural rectification of a high-rise building

Xuedong Cui

Under poor stratum conditions, buildings are particularly susceptible to uneven settlement, which constitutes a significant threat to structural safety. Foundation grouting uplift is generally recognized as an effective method for addressing such issues. This study proposes a novel grouting uplift technology, aiming to overcome some of the deficiencies existing in traditional grouting uplift methods. The technology proposed in this study employs a special high-aluminum iron composite slurry as the grouting material and applies a construction strategy of low-pressure and slow grouting in different areas. For strata with voids, a staged grouting uplift technology (first reinforcement and then uplift) is further formulated to ensure the stability of the strata and the safety of the structure. During the grouting uplift process, automatic monitoring equipment is equipped for real-time monitoring. This technology has been successfully applied to the building settlement control project in Mengshan County, Guangxi, China, achieving excellent results: after the grouting construction was completed, the tilt of the building was reduced from 6‰ to 0.3‰, meeting the requirements for normal use and habitation. During the research process, a detailed geological investigation was first conducted on the site where the building was located. Based on the data obtained from the investigation, a numerical simulation was carried out using the finite difference software FLAC3D, which identified the cavities in the strata as the cause of the uneven settlement of the building and their impact on the building structure. Based on the results of numerical simulation, the feasibility of the grouting uplift construction was analyzed, and a detailed construction plan was formulated. Finally, based on the field monitoring data after construction, the application effect of this new grouting lifting technology was evaluated, and its future development direction was discussed.

Keywords Building settlement, Grouting uplift technology, Foundation reinforcement, Numerical analysis

With the acceleration of urbanization, high-rise buildings have become the mainstream of urban construction to address land scarcity. However, high-rise structures impose stringent requirements on foundation bearing capacity and stability, and uneven settlement of raft foundations—one of the most commonly used foundation forms in high-rise buildings—has emerged as a critical post-construction challenge. Unlike combined pile-raft foundations that leverage the synergistic bearing of piles and rafts to enhance stability, standalone raft foundations are more prone to insufficient bearing capacity when constructed on weak strata, leading to differential settlement after completion. Such settlement not only impairs the building's service performance but also poses severe threats to structural safety: when the tilt rate exceeds 4‰, occupants may experience discomfort, and a tilt rate of 7‰ or higher raises the risk of structural collapse^{1–3}—a threshold widely recognized in engineering standards such as the Chinese national standard GB 50,007 – 2011, Code for Design of Building Foundation⁴. Given the dense population and traffic in urban areas, uneven settlement of high-rise buildings can trigger catastrophic consequences, making the development of effective post-construction rectification technologies urgently necessary.

Grouting uplift has been proven as a reliable technique for addressing building settlement and tilt, particularly for rectifying settled structures with raft foundations^{5,6}. This method stabilizes strata and compensates for settlement by injecting grout into the underlying soil, thereby lifting the structure. Previous studies have focused on optimizing grouting parameters and verifying application effects for specific scenarios: Ni et al.⁶ utilized fracture grouting to correct tilt in clayey sand strata, demonstrating that real-time monitoring of basement column elevations can effectively track uplift and post-grouting settlement. Liao et al.⁷ conducted field tests in Shanghai's saturated soft clay to identify key factors influencing grouting efficacy, providing a reference for parameter design in soft soil environments. Bai et al.⁸ confirmed that grouting uplift is the most widely used and effective measure among techniques for controlling building settlement adjacent to construction sites.

Beijing Hengxiang Hongye Foundation Reinforcement Technology Co., Ltd, Beijing 100097, China. email: hengxianghongye@126.com

These studies have laid a foundation for the application of grouting uplift in building rectification, but critical challenges remain unresolved.

The core challenges of grouting uplift for post-construction high-rise buildings with raft foundations include three aspects: (1) Synchronous uplift control: Due to the heterogeneity of weak strata and the uncontrollable diffusion of traditional grouts, achieving uniform uplift of the entire structure is difficult, which may induce additional deformation or cracking of the foundation slab and superstructure. (2) Material limitations: Conventional cement-based grouts suffer from uncontrollable curing times, excessive volume shrinkage during solidification, and limited diffusion range, leading to local re-subsidence after rectification and compromising long-term stability^{5,6}. (3) Lack of integrated diagnostic-design methodologies: Existing studies often separate geological investigation, settlement cause analysis, and grouting scheme design, failing to establish a systematic link between stratum characteristics (e.g., cavities, weak zones) and grouting strategies, which affects rectification accuracy and safety.

Numerical simulation plays a pivotal role in optimizing grouting uplift schemes by predicting structural responses and verifying feasibility. Two primary simulation approaches are widely adopted: volume strain application and pressure loading. Ni et al.⁹ used PLAXIS2D to simulate grouting uplift by applying volume strain to grouted elements, validating the method's reliability through comparison with field measurements. Zhang et al.¹⁰ proposed a FLAC3D-based simulation technique that applies radial velocity to grouting hole boundaries, enabling efficient simulation of grout expansion in complex geometric regions without iterative trials. Schweiger et al.¹¹ enhanced element stiffness in grouted and affected zones to simulate uplift effects, achieving accurate reverse analysis of the grouting process. Although these numerical methods have enhanced the scientific rigor of design schemes, few studies have integrated numerical simulation with geological diagnosis and real-time field monitoring to establish a closed-loop, feedback-driven design methodology for post-construction rectification of high-rise buildings with raft foundations on weak strata.

Despite progress in grouting uplift technology, research gaps persist in addressing the specific demands of post-construction rectification for settled high-rise buildings with raft foundations: (1) Existing grouting materials cannot simultaneously meet the requirements of controllable curing time, minimal shrinkage, and adjustable diffusion range, limiting their adaptability to complex weak strata. (2) Traditional single-stage grouting strategies lack targeted measures for strata with cavities or weak zones, increasing the risk of uneven uplift and structural damage. (3) Integrated diagnostic-design frameworks that combine geological investigation, numerical simulation, and real-time monitoring are insufficiently developed, leading to scheme design that is disconnected from actual stratum conditions.

To address these limitations, this study proposes a novel grouting uplift technology for post-construction rectification of raft-foundation high-rises on weak strata, taking the settled building in Mengshan County, Guangxi, as a case study. The research sequence is as follows: first, a comprehensive geological survey is conducted to identify settlement causes (e.g., strata cavities, weak layer distribution); second, a FLAC3D numerical model is established to analyze the mechanical response of the structure and evaluate the feasibility of grouting uplift; finally, a tailored scheme is developed, incorporating a high-aluminum iron composite grout with controllable properties and a staged “reinforcement-first, then uplift” strategy. Real-time automatic monitoring is integrated throughout the construction process to ensure synchronous uplift and structural safety. This study aims to provide a systematic and reliable solution for post-construction rectification of similar high-rise buildings, filling the existing knowledge gaps in integrated diagnostic-design methodologies and advanced grouting materials.

Comprehensive diagnosis and monitoring analysis of settlement causes Site overview and geological conditions

Project overview

The project is located in the southern part of Mengshan County, Wuzhou City, Guangxi, on the east side of G321 National Highway and south of Huahong Binjiang New Town, as shown in Fig. 1. The site was originally a vacant lot, and during the field investigation, it had been mostly excavated and leveled to the basement level, resulting in a spacious, flat area. There was a slight slope to the west, and the elevations of locations throughout the site ranged from 138.21 to 144.03 m, with a relative difference of 5.82 m. During the field investigation, no landslide, abandoned mine area, ground collapse, or other adverse geological phenomena were found within the site or in the surrounding area, nor were any adverse geological actions observed that could affect the stability of the foundation. According to the field investigation, no overhead lines, underground pipelines, or underground optical cables with identifications that could affect the project were found during the survey period.

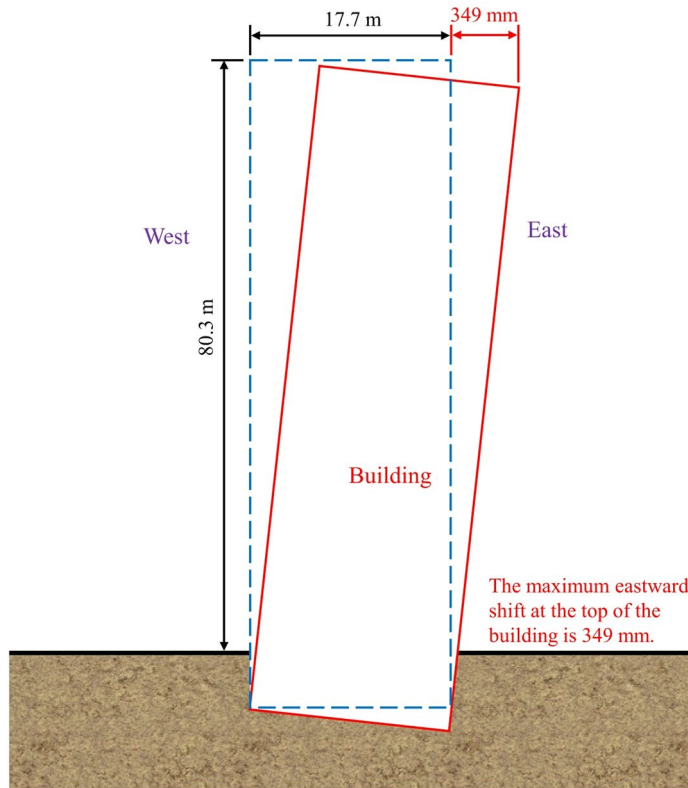
The building is designed with a basement level and 26 floors above ground, measuring 76.98 m in length and 17.7 m in width, with a height of 80.3 m. The ± 0.000 elevation of the building is based on the absolute elevation of 143.55 m. The main structural form of the building is a shear wall, and the basement is a frame structure. The foundation of the building is natural, and the foundation form is a raft foundation, with a raft thickness of 1.3 m and a foundation top elevation of 5.7 m. The bearing stratum is a cobble stratum, with a bearing capacity characteristic value of 300 kPa. After the main structure of the building was topped out, the settlement and tilt of the main structure continued to develop, and the reinforced concrete slab, beams, columns, and walls at the intersection of the main structure and the basement began to crack, with some areas experiencing leaks.

Soil layer distribution

The main fault structure in this region is the Mengshan-Maduang fault belt. This fault belt is located in the area between Yulin City and Meng County, with a total length of about 130 km. The fault belt cut the Cambrian-Tertiary system, and the southern part was the controlling fault of the Cretaceous red fault basin, which made the Cretaceous system contact with the Cambrian Huangdongkou Formation, and continued to develop the Paleogene continental sedimentary basin along the fault. The northern section of the fault belt cuts the near east-



(a)



(b)

Fig. 1. Project profile. This figure was drawn using AutoCAD 2024 (Autodesk, Inc., San Rafael, CA, USA). (a) Location of building, (b) Building schematic diagram.

west Caledonian fold belt, composed of Cambrian flysch series in the middle part of Dayaoshan Uplift, and the fault is multi-phase active and controls the composite fault of the meso-Cenozoic continental sedimentary basin. The proposed site is far away from the fault belt, and no other active faults pass through the surrounding area, and no other fault belt intersects with the Mengshan-Maduang fault belt. As shown in Fig. 2, according to the drilling, karst caves appear in the strata below the building, mainly distributed in the muddy siltstone stratum. The site is composed of quaternary plain fill (Q4ml) and alluvial pebbles (Q3al) from top to bottom, and the

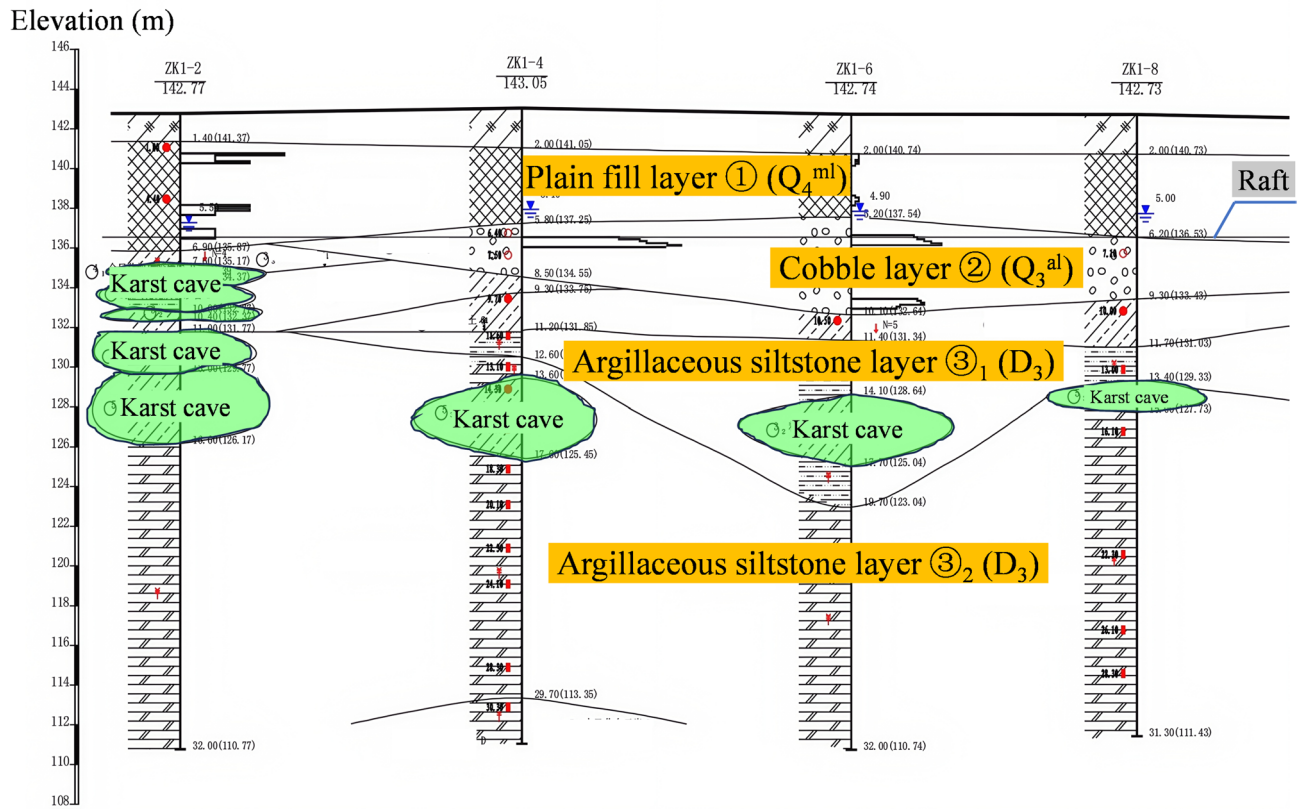


Fig. 2. Schematic diagram of a geological section.

Soil layer	Characteristic
Plain fill layer ① (Q_4^{ml})	Loose in structure, poor in uniformity, and high in compressibility. This layer is distributed on the western surface of the site and is exposed with a thickness of 1.20–3.10 m, with an average of 2.36 m, and a base elevation of 138.26–141.16 m.
Cobble layer ② (Q_3^{al})	Medium-density state, weathered to a moderate degree, with poor sorting. The formation has been exposed in all drill holes, with thickness ranging from 1.80 to 6.40 m, with an average of 3.81 m, and a base elevation of 133.33–136.97 m.
Argillaceous siltstone layer ③ ₁ (D_3)	Strongly weathered, with local patches of complete weathering, clay texture, classified as extremely soft rock, with basic quality grade V. This layer has been exposed in all drill holes, with thickness ranging from 5.90 to 13.30 m, and has been penetrated in the area of high-rise buildings, but not in the area of multi-story buildings.
Argillaceous siltstone layer ③ ₂ (D_3)	Weathered, the rock mass is relatively intact, clay texture, fractures are well developed, it belongs to soft rock, the basic quality grade of the rock mass is Grade IV. There is an exposure within the site in the high-rise building area, with a maximum exposure thickness of 10.50 m, and the layer has not been penetrated.

Table 1. Characteristics of the soil layer.

underlying bedrock is muddy siltstone of the Devonian system (D_3). The characteristics of various strata from top to bottom are shown in Table 1.

Hydrogeologic condition

The building site is located approximately 80 m east of the Meijiang River. According to hydrological data, the 50-year flood level of the Meijiang River near the site is 145.30 m. The site is flat and open, with a leveling elevation of 143.95–144.25 m. The bedrock stratum below the foundation is a cobble stratum, with sand and gravel filling the spaces between the cobbles. The flood has a small impact on the foundation and base of the building site. All the boreholes drilled during this exploration revealed groundwater, which is of the type of intergranular type and exists in the gravel stratum. The initial water level and the stable water level measured during the survey were consistent.

Field monitoring plan and results

Field monitoring scheme

In this study, the building structure was monitored for settlement. Due to the lack of settlement monitoring data during the construction stage of this project, the elevations of characteristic points beneath the basement floor were measured during the research process, and the changes in the elevation of the foundation and the current

state of foundation inclination were determined by comparing with the construction drawings. As shown in Figs. 3 and 22 settlement monitoring points were set up around the building to measure the settlement of the building after construction was completed. There are 8 settlement monitoring points on the west side of the basement roof, 8 on the east side, and 6 in the middle of the basement roof. Continuous monitoring was carried out on the settlement of the building, and the degree of inclination of the building was calculated.

The building monitoring scheme adopted in this study is as follows: based on the site conditions, a level point is selected for level measurement. Additional work points have also been set up for reference point measurement. Based on the specific elevation datum point selected, the work points are arranged together with the monitoring points to form an independent closed loop or a node network formed by compatible routes.

The vertical displacement monitoring points are located on the exterior walls of the building, with an interval of 15 m between them. The arrangement of vertical displacement monitoring points is shown in Fig. 4(a), where K_1 is the distance from the monitoring point to the outer surface of the building, and K_2 is the depth of the monitoring point embedded in the structure. The monitoring points must meet the following specifications: The vertical displacement monitoring points for buildings are made of L-shaped threaded steel, with a recommended diam of 18–22 mm, and the exposed end top should be machined into a ball shape. The markers were buried using a drilling method, and the surrounding voids were tightly filled with grout. The height of the marker should be at least 300 mm above the ground. The distance from the top of the rebar to the outer surface of the building should be 30 mm to 40 mm, and the embedment length of the rebar should be one-third to one-half of the wall thickness.

During monitoring, observations are conducted according to the technical requirements of the vertical displacement monitoring, utilizing geometric leveling measurement methods and a Trimble DINI03 electronic level for observations, as shown in Fig. 4(b). The field monitoring data are recorded using the recording program built into the electronic level. First, determine the elevation of the benchmark, then perform leveling measurements on points within the survey area. Each closed-loop route is driven once, data is recorded, and analyzed. When conducting the initial observation, three consecutive measurements must be taken to ensure the accuracy of the measurement results. The average value obtained is then used as the initial value for the settlement observation point. Measurement sequence: Forward measurement: back, front, front, back; Reverse measurement: front, back, back, front. When monitoring, the angle between the leveling instrument's sight axis and the horizontal plane should not exceed $\pm 15^\circ$. The difference between the main scale and auxiliary scale readings of the level should not exceed 0.15 mm, and the gap between the main line and auxiliary line of the height difference obtained should not exceed 0.7 mm. The degree of building inclination is determined by the ratio of the settlement difference between two endpoints of the building foundation in the direction of preference to the spacing between those two endpoints.

Analysis of field monitoring

After the completion of the high-rise building construction under the focus of this study, due to the closed structure, the monitoring points JZ1-20 and JZ1-22 could no longer be observed. The settlement of the building foundation is shown in Fig. 5. After the building was completed, the cumulative maximum settlement amount was approximately 216 mm, the cumulative minimum settlement was about 50 mm, and the cumulative maximum settlement difference was 166 mm. The settlement in the northwest direction of the building is smaller, while the settlement in the southeast direction is larger. The building structure is tilting towards the southeast direction overall.

Before carrying out the grouting uplift construction, it is of great significance to clarify the overall inclination of the building. Therefore, supplementary monitoring was conducted at the monitoring points shown in Fig. 3 to improve the monitoring data and thereby obtain a more accurate result of the inclination of the building. That is, the data loss of monitoring points JZ1-20 and JZ1-22 occurred after the completion of the building construction. Before the grouting lifting construction began, all monitoring points were re-observed. The overall tilt of the

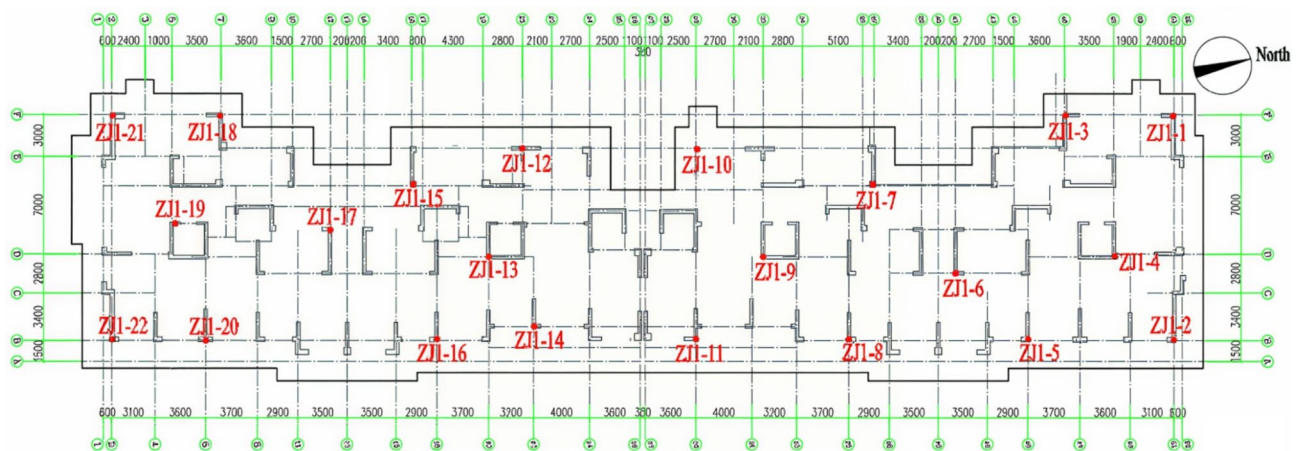
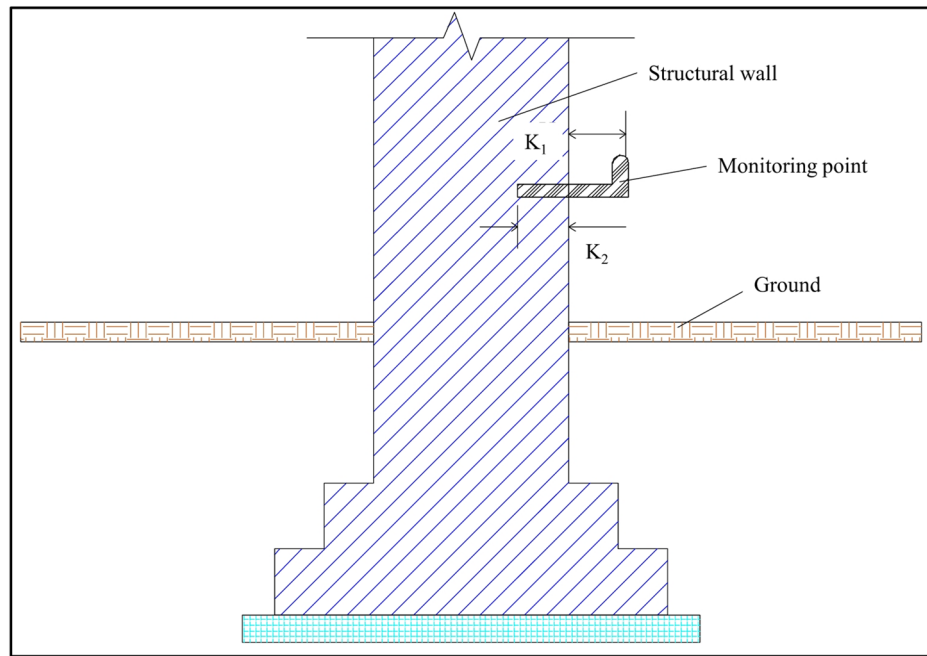


Fig. 3. Layout of measuring points of the building.



(a)



(b)

Fig. 4. Vertical displacement monitoring. (a) Vertical displacement monitoring points for buildings, (b) Schematic diagram of monitoring instruments.

building foundation is shown in Table 2. The location of the monitoring points along the axis is shown in Fig. 3. Based on the results of the topographic survey, the apparent maximum east-west inclination of the building foundation is about 6‰. The overall inclination of the building is 4.65‰ to the east and south. The monitoring results are consistent with the settlement monitoring results of the building, and the inclination exceeds the standard.

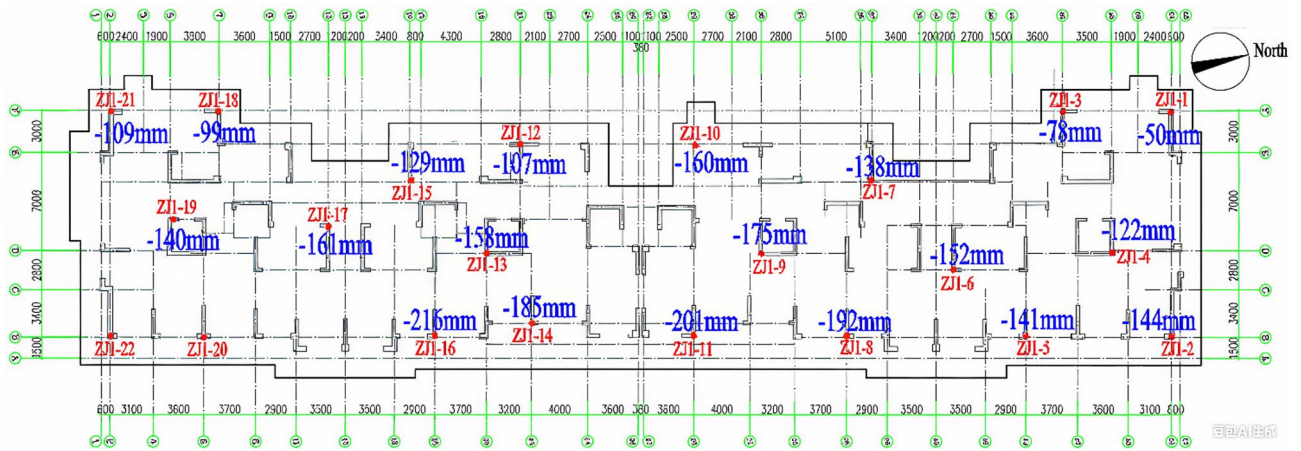


Fig. 5. Monitoring results of the foundation elevation of the building.

Direction of overall inclination	Position of the axis	Number of monitoring points	Differential settlement (mm)	Spacing of monitoring points (m)	Overall inclination (‰)
East-west direction	2	ZJ1-21, ZJ1-22	107	15.9	6.7
	16	ZJ1-15, ZJ1-16	66	10.85	6.1
	23	ZJ1-12, ZJ1-14	81	12.75	6.4
	29	ZJ1-10, ZJ1-11	88	13.0	6.9
	37	ZJ1-7, ZJ1-8	65	11.05	5.9
	46	ZJ1-3, ZJ1-5	105	16.4	6.4
North-south direction	51	ZJ1-1, ZJ1-2	93	16.4	5.7
	D	ZJ1-4, ZJ1-9	-14	22.7	-0.6
	D	ZJ1-13, ZJ1-19	53	25.4	2.1

Table 2. Results of foundation inclination monitoring.

After comprehensively analyzing the geotechnical engineering survey report and the field monitoring, the fundamental reason for the uneven settlement is:

1. According to the geotechnical investigation report and the foundation structural construction drawings, the bearing stratum of the building foundation is the cobble stratum, with a thickness of about 600–800 mm. Because the cobble stratum has a large void ratio, the bearing capacity of the foundation is low, and it is easy for the building to produce uneven settlement. In the process of grouting uplift, this stratum needs to be grouted and reinforced to improve the bearing capacity of the foundation.
2. The weathered fissures in the clay-fine sandstone stratum are well developed, and they easily disintegrate and soften when wet. The core samples are in the form of broken fragments or mud, and it is easy to form underground cavities, which leads to insufficient bearing capacity of the foundation and uneven settlement of buildings above. During the grouting uplift process, it is necessary to fill the cavities in the stratum with grout to strengthen the bearing capacity of the foundation.
3. The high-rise building should adopt a pile foundation or a combination of pile foundation and raft foundation. However, a relatively simple raft foundation was adopted, which is one of the reasons for the uneven settlement. Therefore, it is necessary to reinforce and rectify the foundation of the settlement area to further control the influence of uneven settlement and building lean on the building in the region.

Comprehensive analysis of settlement causes

Establishment of numerical model

To investigate the main causes of building uneven settlement, a three-dimensional numerical model of the building structure was established using the finite difference software FLAC3D, which was divided into the upper structure and lower soil parts as shown in Fig. 6. The superstructure is modeled at actual building dimensions, with a height of 91.6 m, and concrete elements are simulated using a linear elastic model. The soil model has dimensions of 144 m × 60 m × 33.9 m, with the upper boundary being the ground surface, and is simulated using the Mohr-Coulomb plastic model. The model was selected due to its suitability for simulating the elastoplastic behavior of soils under low confinement stress, its simplicity in parameter determination, and its widespread use in geotechnical engineering for simulating soil failure and settlement. We also acknowledge that more advanced models (e.g., Hardening Soil Model) could capture soil hardening behavior but would require more parameters

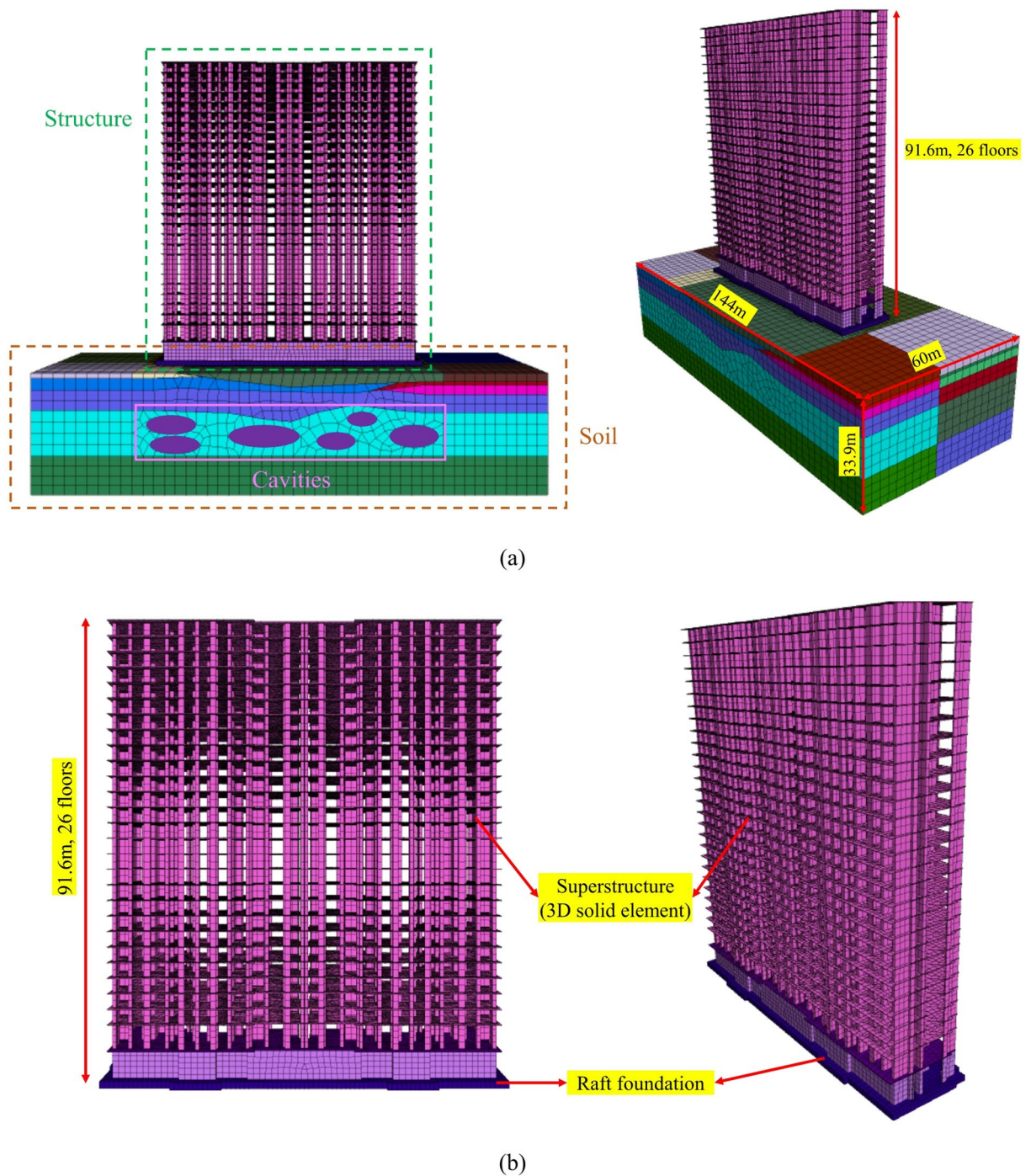


Fig. 6. FLAC numerical model: (a) Simplified numerical modelling; (b) Refined model of the superstructure.

that are not always available from standard site investigations. The voids in the stratum are simulated using an empty model, and their positions and sizes are determined based on engineering geological data obtained from geological exploration. Apply the initial stress to the boundary stress and the body stress of the model. Fix the displacement of the remaining 5 surfaces of the model, except the top surface. The gravity parameter is 9.81 m/s^2 . Based on the geological survey results, the groundwater level is set at 5.5 m above the ground. The 3D numerical model consisted of 57,260 elements and 62,216 nodes. The mechanical parameters adopted for soil and structure are listed in Table 3.

Simulation of building settlement

The numerical simulation results of building settlement are shown in Fig. 7. The maximum cumulative settlement at the bottom surface of the basement roof is approximately -243.56 mm , and the maximum settlement occurs at the east-southeast position of the building structure. The cumulative minimum settlement

Param	Material type	Density (kN/m ³)	Elastic modulus (MPa)	Poisson's ratio	Internal friction angle (°)	Cohesion (kPa)	Thickness (m)
Soil	Plain fill layer	18	9.4	0.32	10	10.00	3.9
	Cobble layer	20.0	22.1	0.30	32	6	4.6
	Argillaceous siltstone layer 1	22.0	30	0.4	24	15	13.8
	Argillaceous siltstone layer 2	22.0	34	0.4	26	17	11.6
Structure	C30	24.0	30,000	0.2	–	–	–

Table 3. Param of numerical simulation.

is approximately – 36.91 mm, and the minimum settlement occurred at a west-northwest position of the building structure. The cumulative maximum settlement difference of the building is 206.65 mm, and the settlement value of the building gradually increases from west-north to east-south. The building tilts to the east-south direction overall, which is consistent with the conclusion drawn from the field monitoring results. From the numerical simulation results, it can be seen that the building settlement is greatly affected by the strength of the stratum, and the building structure tends to lean towards the direction of the weak stratum.

To further verify the reliability of the numerical simulation results, monitoring points were set up in the numerical model to obtain more precise building settlement values. The positions of the monitoring points in the numerical model were consistent with those of the field monitoring points, as shown in Fig. 7(a). As shown in Fig. 7(b), the numerical simulation results were compared with the actual monitored settlement results of the structure, and a good fit was found between them. The root mean square error (RMSE) value between the numerical simulation results and the actual monitoring values is 5.3056, which means that the average error between the two values is approximately 5.3056 mm.

Before the grouting uplift construction began, the maximum eastward displacement of the building top was 349 mm, and the maximum inclination was 4.37%. As shown in Fig. 8, the inclination of the building is consistent with the actual field monitoring results.

According to the results of the field investigation, the steel-reinforced concrete slab, beams, columns, and walls at the intersection of the building's main structure and the basement have cracks, some of which are leaking; some of the cast-in-place concrete components have evidence of injection-based repair; and there is a pooling of water on some unfinished foundation lots. Cracks are the most obvious sign of building deformation. Uniform settlement of the building structure leads to a redistribution of the load on the main body of the building, and shear walls not only bear the vertical load but also bear part of the shearing force, resulting in large cracks appearing on the underground floor walls and the roof of the building. Under the influence of the inclination direction of the building, the development of shear wall cracks has a certain directionality. The change of wall stress is the main factor for crack formation. The farther away from the point of maximum settlement, the greater the moment applied to the wall, and the more developed the cracks. The stress contour plot of the building structure obtained from numerical simulation is shown in Fig. 9. After structural uneven settlement occurs, the principal stress at the walls and the slab of the basement of the building exceeds the concrete ultimate tensile strength value (3.0 MPa), leading to cracking of the building structure. According to the settlement situation of the building and the stress distribution obtained from numerical simulation, the settlement of the building foundation has a small impact on the upper structure and mainly affects the underground structure. The observed cracking situation from the site also supports this point. There are cracks in the underground structure, but no cracks in the upper structure, which is consistent with the observed cracking situation of the building, as shown in Fig. 9(a) and (b). The stress distribution changes that occur after a building subsides are the main reason for the building's structural cracking.

Furthermore, it is worth noting that numerical simulation analysis has found that the nonuniform settlement of buildings seems to be related to the positions of the ground voids, which means that ground voids may be one of the important causes of the nonuniform settlement of buildings. Stratum conditions have a significant impact on the stability of actual engineering projects^{12–15}, among which stratum cavities are one of the key factors affecting stratum stability^{16–18}. To further investigate the influence of ground void on nonuniform settlement of building, numerical simulations of building settlement were conducted under the condition of stratum without void, and the results were compared with those of building settlement under the condition of stratum with void, as shown in Fig. 10. It is worth noting that both scenarios (with and without voids) were simulated under the same stratigraphic conditions. The comparison results show that the settlement value of buildings in the condition without void is lower than that in the condition with void, and the unevenness of building settlement is weaker, with the maximum settlement difference being only 72 mm. The maximum settlement value of the building occurred at the southeast corner of the building, and the minimum settlement value occurred at the northwest corner of the building. Building settlement is affected by the strength of the underlying stratum. The soft stratum below the building has caused the building to settle, and the stratum strength in the southeast corner is less than that in the northwest corner. However, one of the reasons for uneven settlement of buildings is ground void, so attention should be paid to grouting filling of the voids during the raising of the foundation.

Building a grouting uplift scheme design

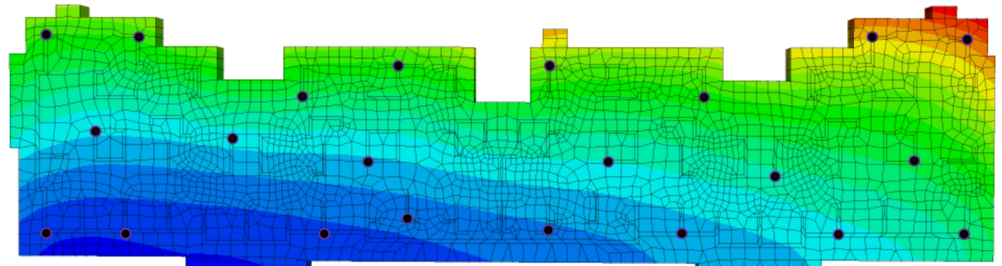
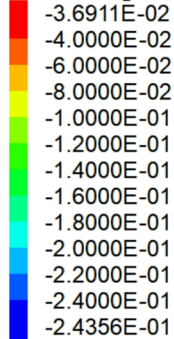
Building the grouting uplift principle

The effect of grouting uplift on the stratum mainly lies in the improvement and consolidation of the stratum, as well as the compensation for stratum loss. The principle of ground consolidation grouting is to push out and replace the pore water in the stratum with the grout injected into the stratum, binding the soil particles into large

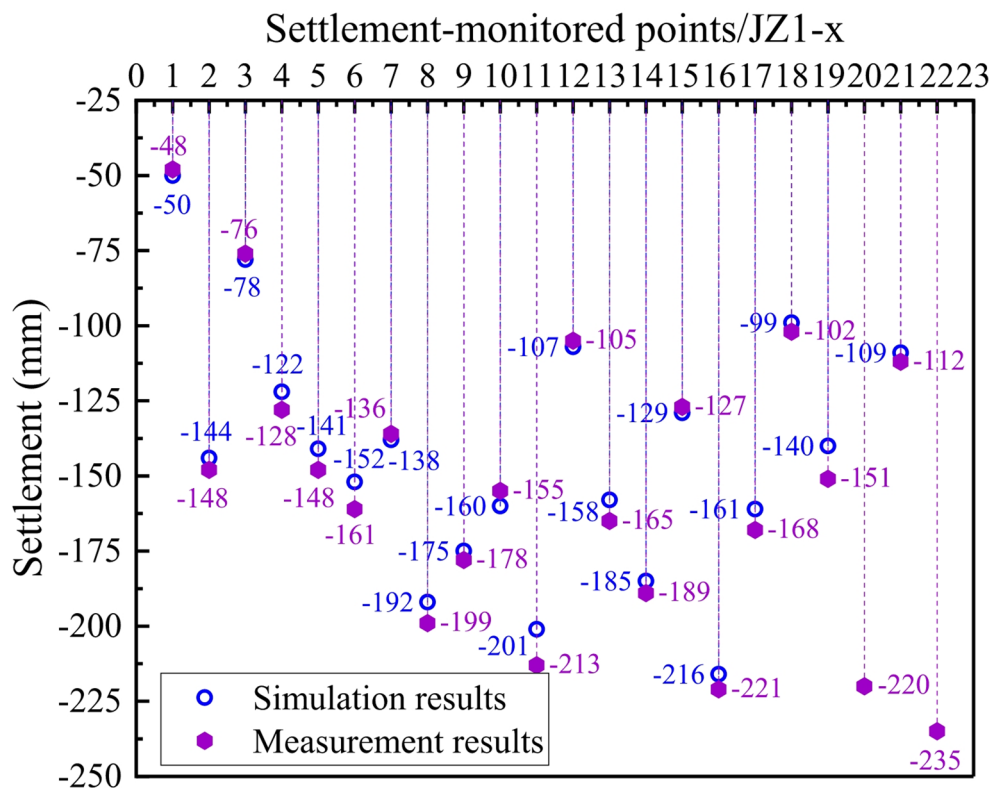
FLAC3D 6.00

©2019 Itasca Consulting Group, Inc.

Zone Z Displacement



(a)



(b)

Fig. 7. Analysis of building settlement. (a) Numerical simulation results of building settlement, (b) Comparison between the results of numerical simulation and field measurement.

cohesive bodies, increasing the stiffness of the soil, and thus achieving the purpose of reinforcing the stratum. Figure 11 shows a model of soil volume expansion caused by grouting, which assumes a spherical region around the grouting point with a radius of a , where the volume before grouting is V_0 and the volume increases by ΔV_0 (compaction grouting is the volume of grout bubbles; fracture grouting is the sum of the volume of the fractured grout liquid in the area). The total volume after grouting is $V_0 + \Delta V_0$. The volume of soil expansion may be isotropic ($\Delta a_x = \Delta a_y = \Delta a_z$), or anisotropic ($\Delta a_x \neq \Delta a_y \neq \Delta a_z$).

Golleger¹⁹ studied the displacement field caused by compensation grouting based on the grouting displacement solution proposed by Sagaseta²⁰. The solution for grouting displacement is shown in Fig. 12.

According to the method of displacement solution calculation²¹, the surface displacement due to grouting is:

The maximum eastward shift at the top of the building is 349mm.

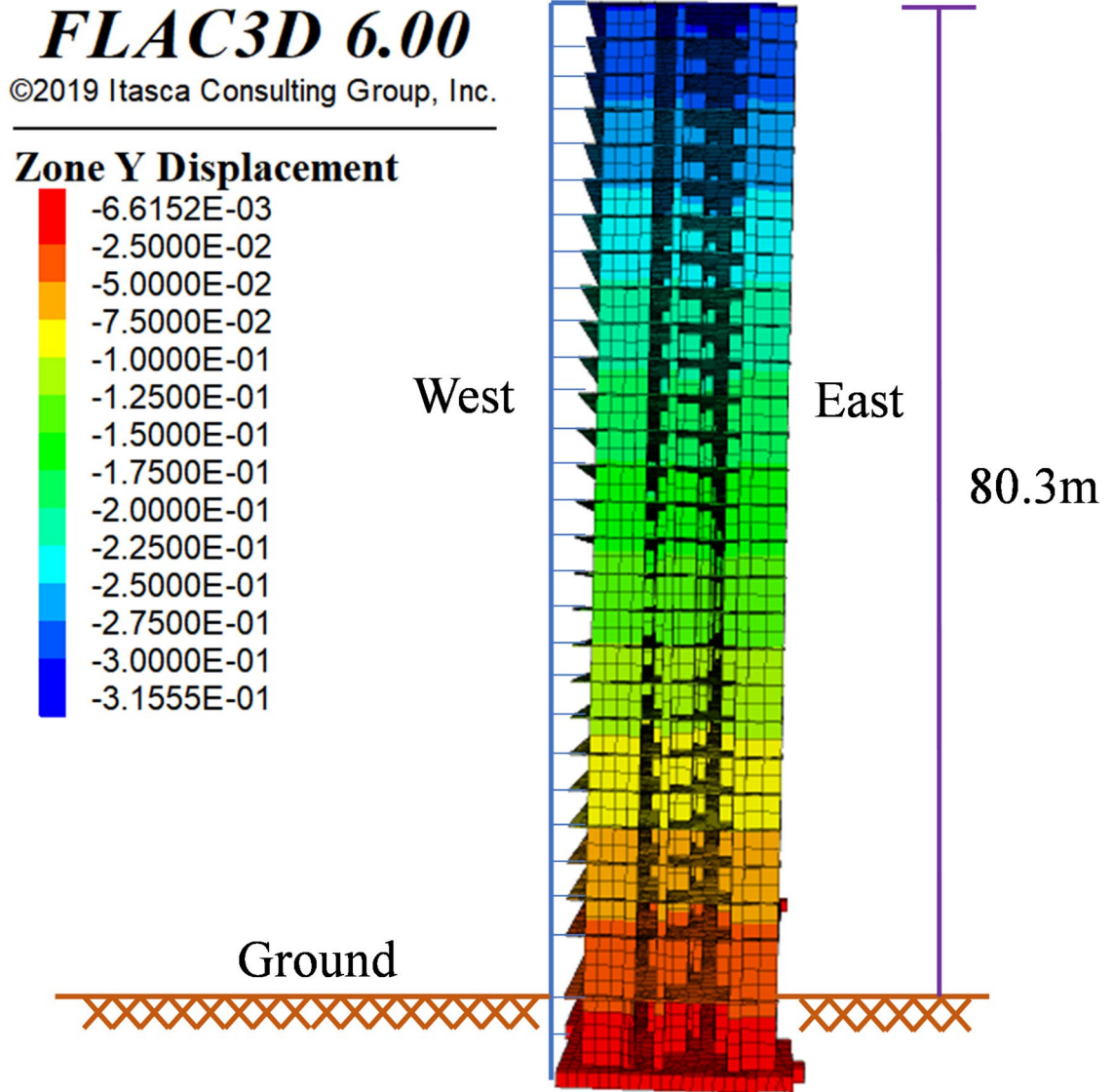


Fig. 8. The building inclination before grouting uplift.

$$s_x = -2\varepsilon \left(\frac{a}{h}\right)^{2a-1} \frac{x'}{(1+x'^2)^a} \left(1 + \rho \frac{1-x'^2}{1+x'^2}\right) \tag{1}$$

$$s_z = 2\varepsilon \left(\frac{a}{h}\right)^{2a-1} \frac{1}{(1+x'^2)^a} \left(1 + \rho \frac{1-x'^2}{1+x'^2}\right) \tag{2}$$

Where: x' represents the ratio of the distance from the grouting point to the center to the burial depth h ; ρ is the relative pseudoplasticity, which is the ratio of the deformation volume in the grouting area to the strain; a is the coefficient of permeability (drainage conditions will affect the volume strain). Depending on the drainage conditions, $a=1.0$ to 1.5 ; when it is an undrained condition, $a=1.0$.

The conventional single-stage grouting uplift correction technology directly injects the grout into the soil mass. The controllability of grouting is compromised by grout fracturing and subsequent infiltration into adjacent weak soil strata. Moreover, the conventional single-stage tilting correction technology cannot be repeated for grouting, and during grouting, excessive static pore pressure is often generated. Even after the void water pressure dissipates, the building will still experience uneven settlement. However, segmented grouting

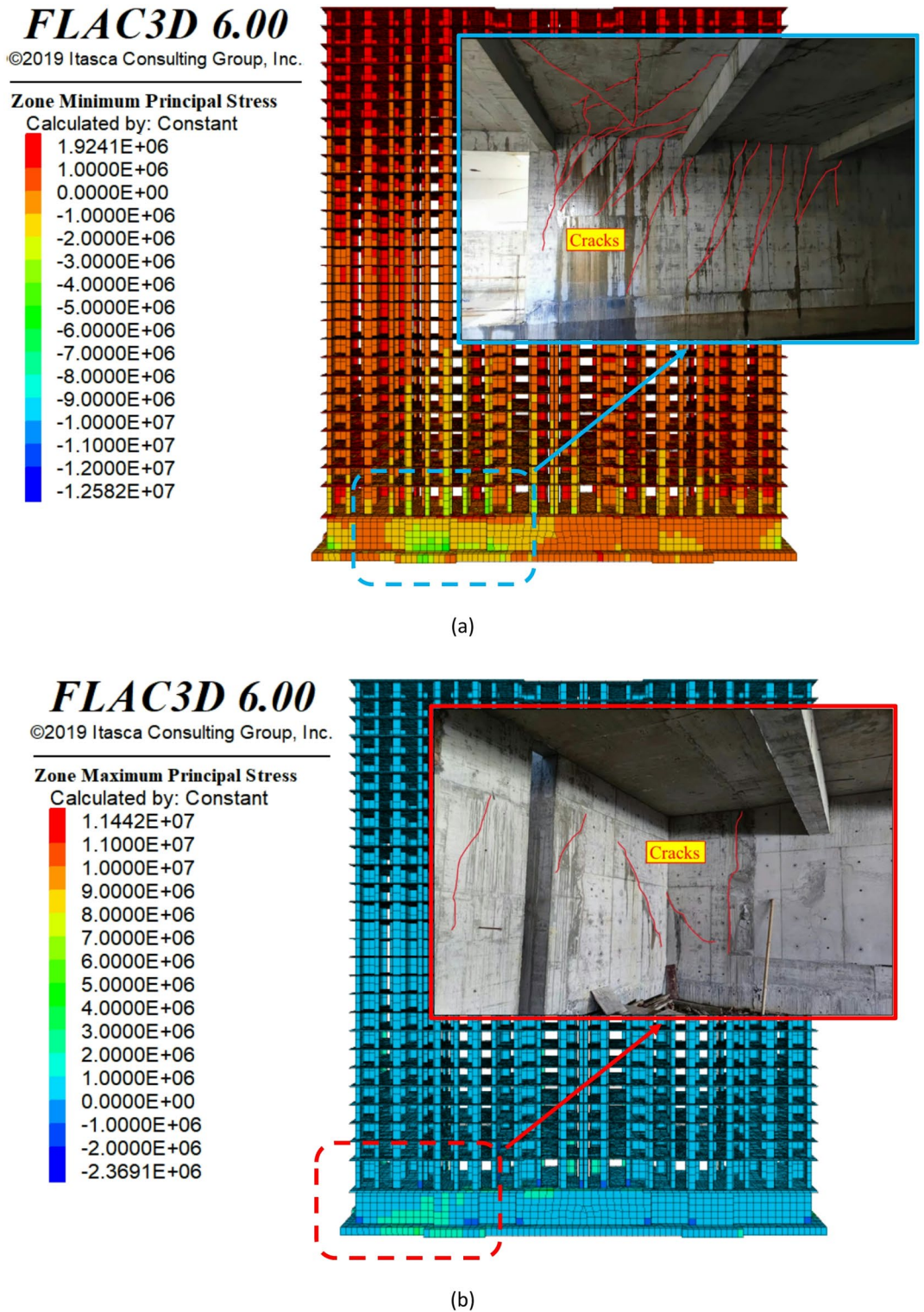


Fig. 9. Numerical simulation results of structural stress. (a) The minimum principal stress caused by building settlement, (b) The maximum principal stress caused by building settlement.

can overcome this limitation. In this study, the building grouting uplift construction integrates the grouting reinforcement technology and the flexible grouting uplift technology, as shown in Fig. 13.

The grouting uplift scheme is divided into two stages for implementation:

Phase 1: Foundation filling and reinforcement stage. This stage mainly involves consolidating and reinforcing the cobblestone layer below the foundation base and the shallow area of the clayey soil, filling the voids in the foundation base, and improving the strength and stiffness of the area to prevent settlement and ensure that

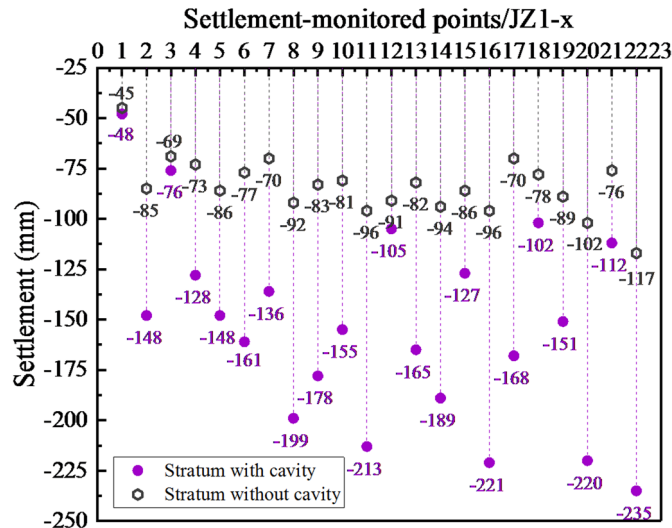


Fig. 10. Comparison between simulation results of building settlements with voids in the stratum.

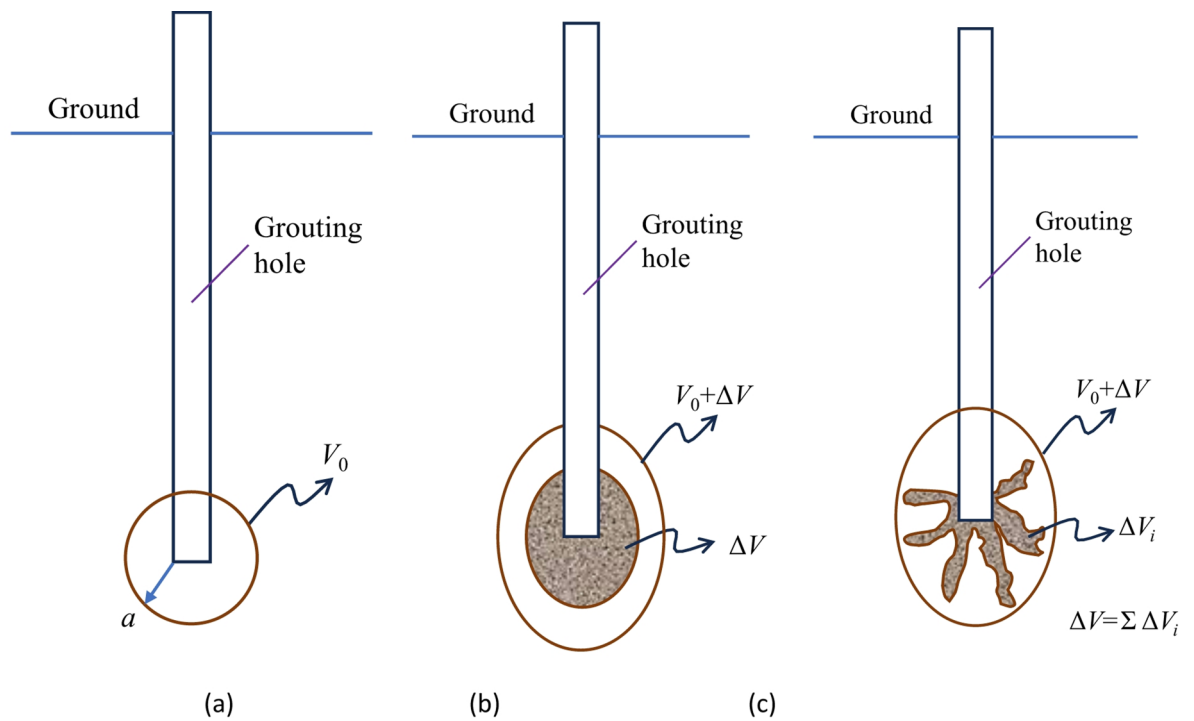


Fig. 11. Basic modeling of soil volume expansion caused by grouting. (a) Grouting range, (b) Pressure grouting, (c) Fracture grouting.

the foundation base receives even loads. Furthermore, grouting consolidation can avoid potential risks such as secondary tilting of the building or tearing of the foundation due to excessive uplift in local areas, thereby ensuring better uplift effects, as shown in Fig. 14.

Phase 2: Foundation grouting uplift stage. After the foundation filling and reinforcement stage is completed, drilling continues downward to the strong weathered dolomite and through the cave, with the slurry being injected into the foundation through the layered retreat reinforcement process. The slurry is driven into the foundation under pressure to fill the cave and the fractures in the bedrock. As the grout fills and compacts, the pressure within the grout rises, causing the material to split, as shown in Fig. 15(a). Vertical forces begin to take effect, causing the building to lift, as shown in Fig. 15(b). According to the project's characteristics, the foundation reinforcement will be carried out using the drilling and injection process in a retreating manner, to meet the requirements of the foundation's bearing capacity.

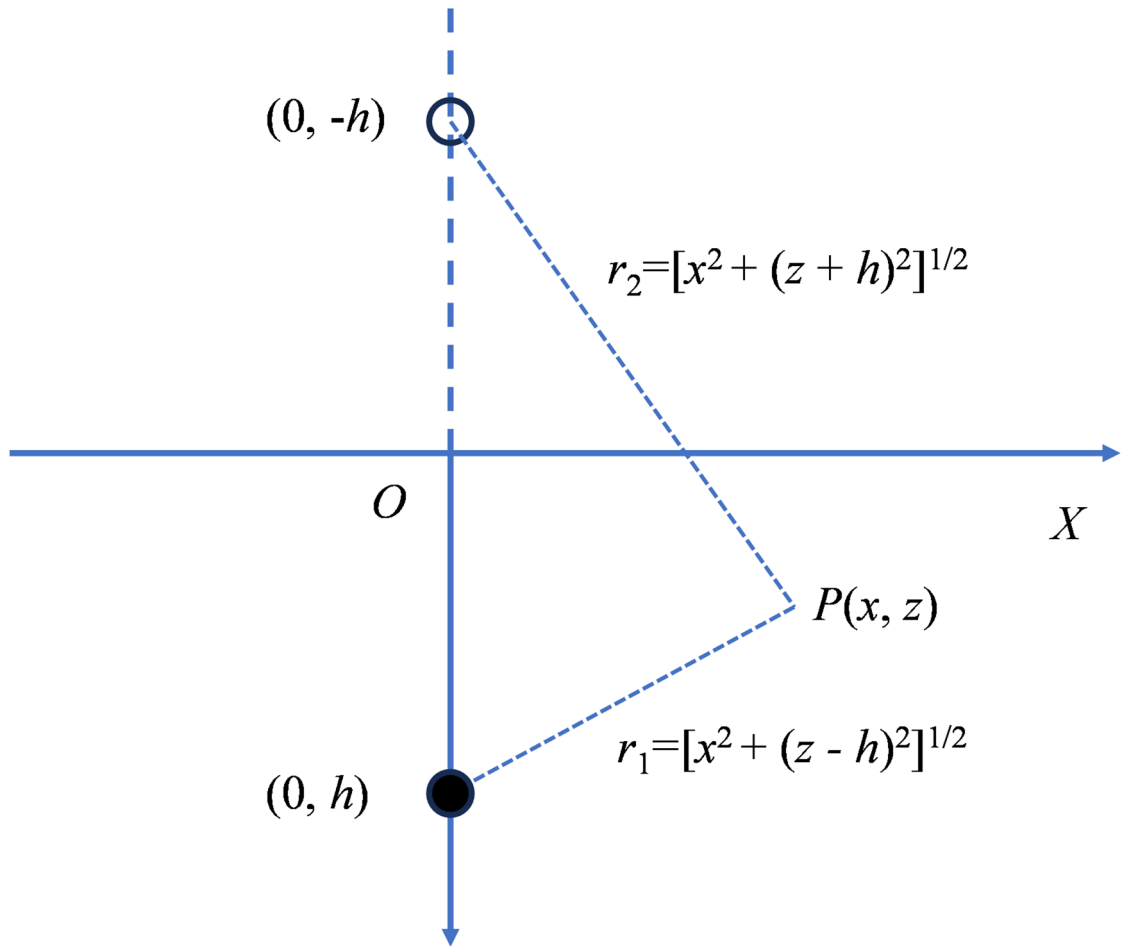


Fig. 12. Schematic diagram of displacement solution.

Building grouting uplift scheme

Grouting hole positioning

As shown in Fig. 16(a) and (b), according to the actual conditions on site, the reinforcement holes (lifting holes) are arranged.

Reinforced hole arrangement and depth: Based on the structural form and slope direction of the building, which is inclined to the east, the drilling method is mainly divided into outdoor drilling (the grouting drilling carried out in the stratum located inside the building outline) and indoor drilling (the grouting drilling carried out in the stratum located outside the building outline). The outdoor holes are mainly located on the east and west sides of the building. The drilling principle is to position the holes corresponding to the shear walls along the axis line. The east hole is located about 2.7 m away from the outer wall, and the drilling angle is about 7 degrees. The depth is about 26.5 m. The west hole is located about 1.7 m away from the outer wall, and the drilling angle is also about 7 degrees. The depth is controlled to enter the strong weathering dolomite at least 1 m deeper than the report and to reach 21.3 m. The depth of the indoor hole is 21.3 m. The hole positions and depths should be adjusted according to the actual site conditions and avoided near shear walls.

Lifting holes: Lift the building on the side with a larger settlement volume (east side, south side) by utilizing the original reinforced holes. The lift side can be appropriately densified according to the actual situation on site.

Grouting reinforcement area

As shown in Fig. 17, this project involves full-area reinforcement of the foundation beneath the building, with the reinforcement area extending 1.0 m beyond the outline of the foundation. The reinforcement area has a total floor area of approximately 1664 m². The overall reinforcement depth is 20.0 m below the bottom of the raft foundation. The raft composite foundation reinforcement area is 1664 m², the reinforcement depth is 20.0 m, and the reinforcement volume is approximately 33,280 m³.

Grouting technical parameters

The grouting uplift parameters adopted in this project are shown in Table 4. These parameters are consistent with the uplift response observed in the actual application of this study and the engineering practice of previous successful cases²².

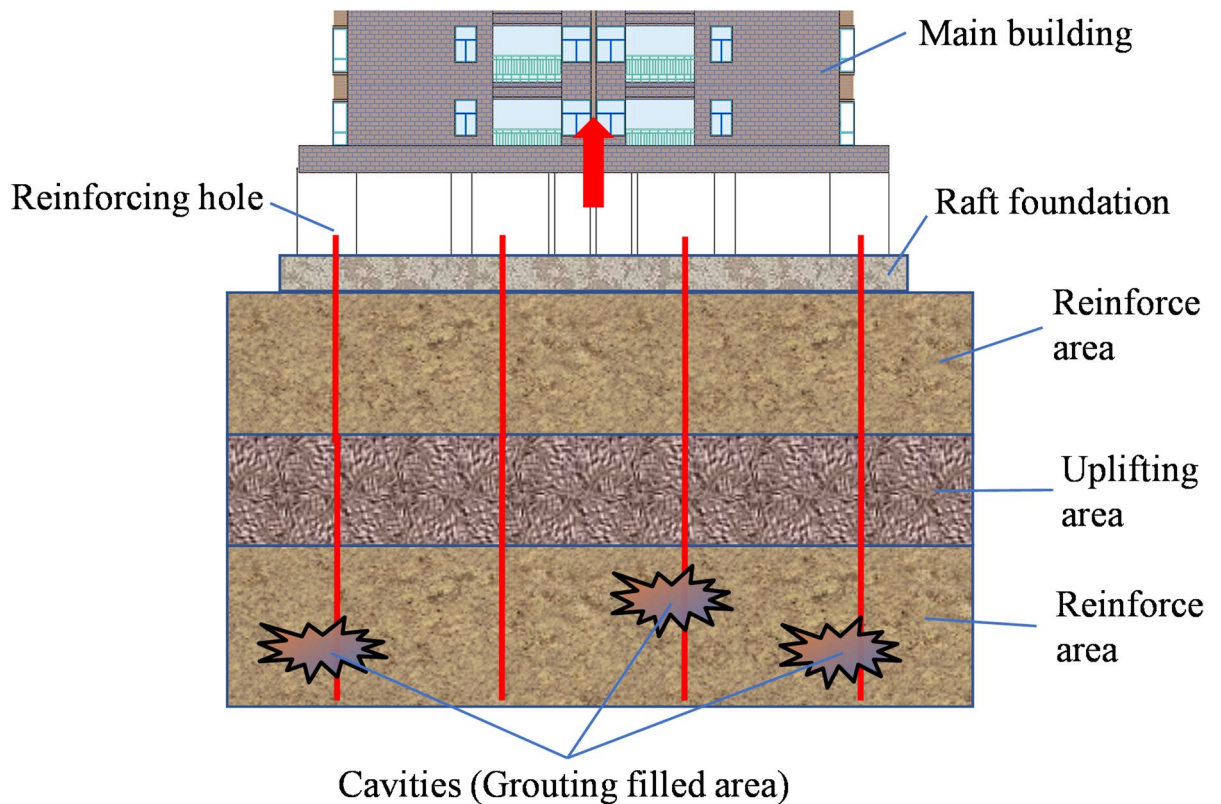


Fig. 13. Schematic diagram of the building grouting uplift.

Grouting material selection

A large number of researchers have conducted studies on grouting materials^{21,23–27,30}. To successfully implement the project and achieve the goal of consolidating the foundation and lifting the deviation, a special high-aluminum iron composite slurry will be selected. This slurry is mainly composed of aluminum slag and iron slag. Aluminum slag primarily serves to accelerate setting, while iron slag mostly enhances strength and durability. It belongs to the category of cement-based materials and is a modification of traditional high-alumina iron cement materials. Through a large number of indoor experiments, we have obtained the optimal proportion of the high-aluminum-iron special composite slurry (aluminum slag: iron slag: cement = 3:2:1 by weight), and its unconfined compressive strength at 28 days is no less than 48 MPa. After solidification, the structure formed by the slurry has high strength and strong impermeability, and the bearing capacity of the foundation is significantly improved.

Technical characteristics of engineering materials: (1) The curing time can be easily adjusted, and the curing time of the slurry can be controlled within 10 s to 90 s; (2) The spreading range can be controlled within a radius of 2.5 m, breaking the technical limitation of uncontrollable slurry materials in traditional methods; (3) It has good permeability and can have a strong penetration ability for a fine sand stratum. After hardening and setting, it has high strength; (4) It also has a very strong consolidation performance in water-rich formations and confined aquifer formations; (5) The shrinkage rate after curing is less than 0.02%, and the hardener is non-toxic, so it will not contaminate groundwater.

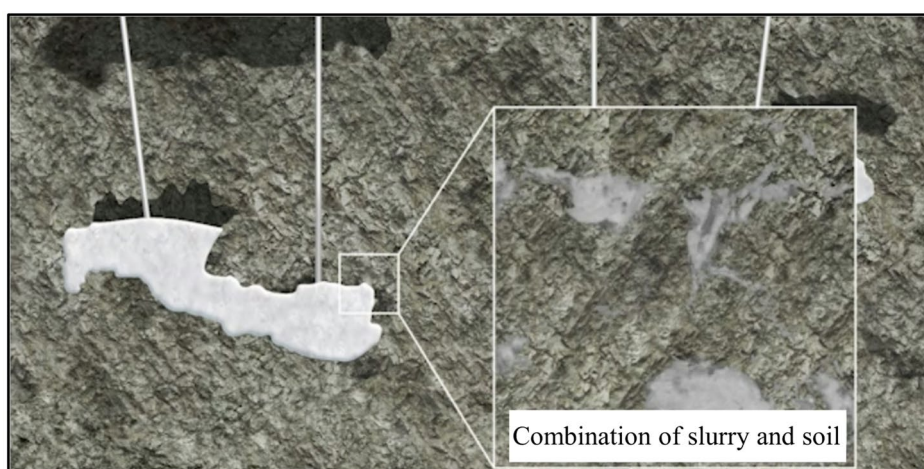
Grouting construction process

According to the settlement data of the basement roof elevation measurement and the foundation inclination data, the maximum inclination of the foundation of the building is about 6‰, and the target inclination is controlled at 2.0‰. The calculated maximum controlled uplift on the east side is 130 mm, which gradually changes along the west side. The final lifting height should be determined according to the actual site inclination and the safety and stability of the superstructure. Implement according to the field retest value. In the actual lifting process, 10 sets of equipment were selected to lift at the same time. In the process of lifting, 10 sets of equipment are used to carry out the flow operation at the same time, from the part with large settlement value to the part with small settlement value, and the lifting process is equipped with automatic monitoring instrument for real-time monitoring; According to the Code for Design of Building Foundation (GB-50007-2011)¹⁷, the ratio between the settlement difference at both ends of the foundation and the distance between them should not be greater than 0.0025, and the calculated maximum lifting height per cycle should not be greater than 30 mm, and the maximum lifting height per day should be 3–10 mm.

Construction is recommended from the area with large settlements to the area with small settlements, and construction is carried out from outside to inside. As shown in Fig. 18, this project adopts the backward



(a)



(b)

Fig. 14. Schematic diagram of grouting reinforcement.

grouting process. In the construction process, the grouting slurry is mixed first, and then the backward grouting is carried out gradually upward from the bottom of the hole. The lifting hole is implemented by using the original reinforced hole.

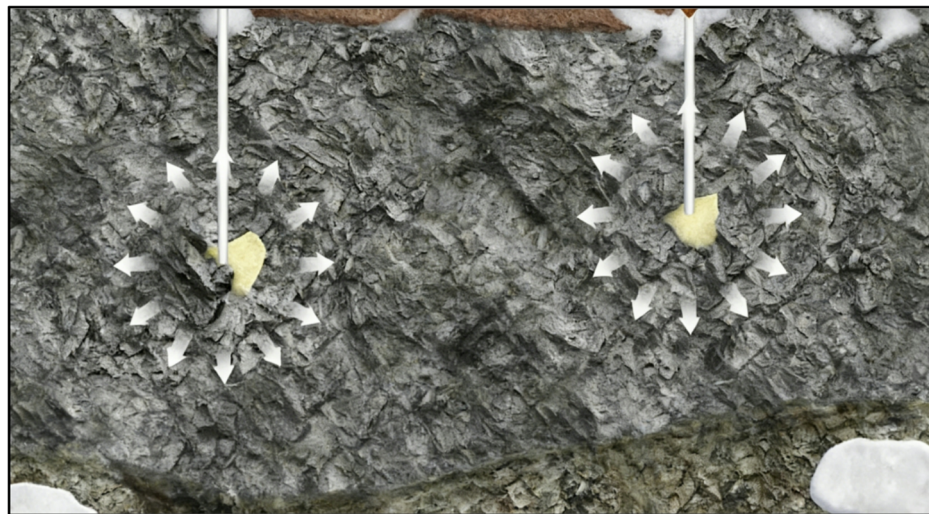
The grouting uplift process is shown in Table 5.

Scheme feasibility analysis

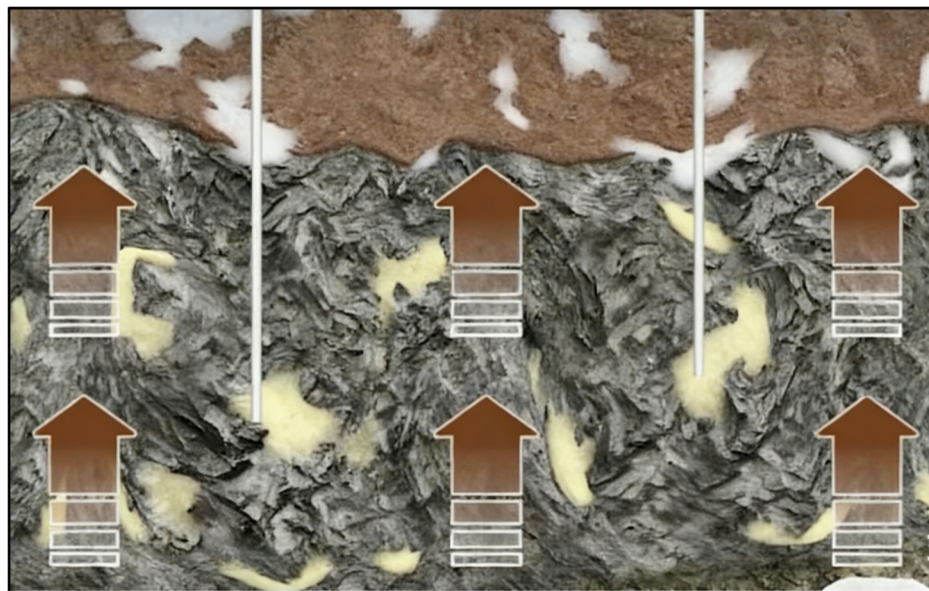
Numerical simulation scheme

It can be concluded from the analysis of settlement causes that building settlement is caused by the combined action of soft soil layers and voids in the soil, and the main reason for uneven settlement of buildings is the appearance of soil voids. To verify the feasibility of the ground foundation grouting uplift scheme, the impact of grouting uplift construction on buildings was studied numerically. The research results show that isotropic expansive pressure can be applied to simulate pressure grouting, and anisotropic expansion pressure can be used to simulate pressure grouting and fracture grouting²⁸. This study used FLAC3D to apply isotropic expansive pressure to the elements, causing them to expand in volume, thereby simulating the lifting process of grouting. In the numerical simulation, the shallow consolidation area, deep consolidation area, and injection lifting area were set, as shown in Fig. 19.

The numerical simulation of the grouting uplift process is based on the simulation results of uneven settlement of the building. First, the voids in the strata are filled with grout, and the weak soil layers are reinforced. Then, the grout pressure is applied to the area where the grout lifting has taken place. In the actual construction process, the soil in the soil consolidation area will not cause the building structure to rise. In the numerical simulation,



(a)



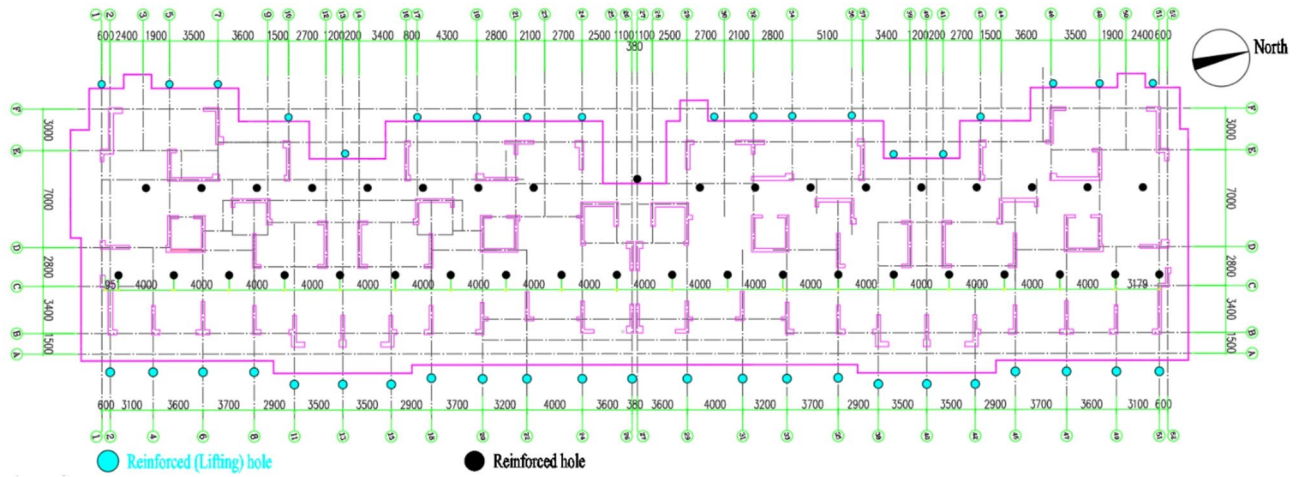
(b)

Fig. 15. Schematic diagram of grouting uplift.

the shallow consolidation area soil and the deep consolidation area soil are replaced with grouted solid (the grouted consolidation area is referenced in Fig. 19). It should be noted that voids in the geological layers need to be reset to elastic constitutive material models. The grouted reinforcement material is selected with an elastic constitutive material model, and the elastic modulus of the rock layer is taken as 1 GPa²⁹. In the actual grouting process, it is recommended to use a grouting pressure of 0.3–1.5 MPa. The grouting pressure at each injection hole position should be adjusted according to the actual construction situation to ensure the normal operation of the grouting process. In numerical simulations, for the convenience of calculation, the grouting pressure for different grouting holes was simplified, and the expansive pressure in the grouting consolidation area was set to a fixed value. Because it is impossible to determine whether the grouting process is completed by applying expansive pressure on the element, in this numerical method, the grouting process is controlled by judging whether the volume strain increment of the element is equal to the volume strain increment of the soil. The volumetric expansion of the soil will result in an uplift of the ground surface, as illustrated in Fig. 20.

Assuming a proportional relationship between the volume of soil expansion and the volume of grouting:

$$\xi = V_{sh}/V_{inj} \quad (3)$$



(a)



(b)

Fig. 16. (a) Schematic diagram of grouting hole locations; (b) Grouting equipment.

where: ξ represents the grouting compensation rate; V_{sh} represents the volume of soil expansion; V_{inj} denotes the volume of grouting. ξ is not a constant during grouting, and its value is affected by geological conditions, stress levels, and consolidation history, among other factors. Furthermore, after a period of grouting, the value of ξ decreases due to soil consolidation. Research and experience have shown that the value of ξ is generally between 5% and 20%. According to Eq. (3), the volume strain of the soil is defined as:

$$\Delta\varepsilon_V = \frac{\xi V_{inj}}{V_0} \tag{4}$$

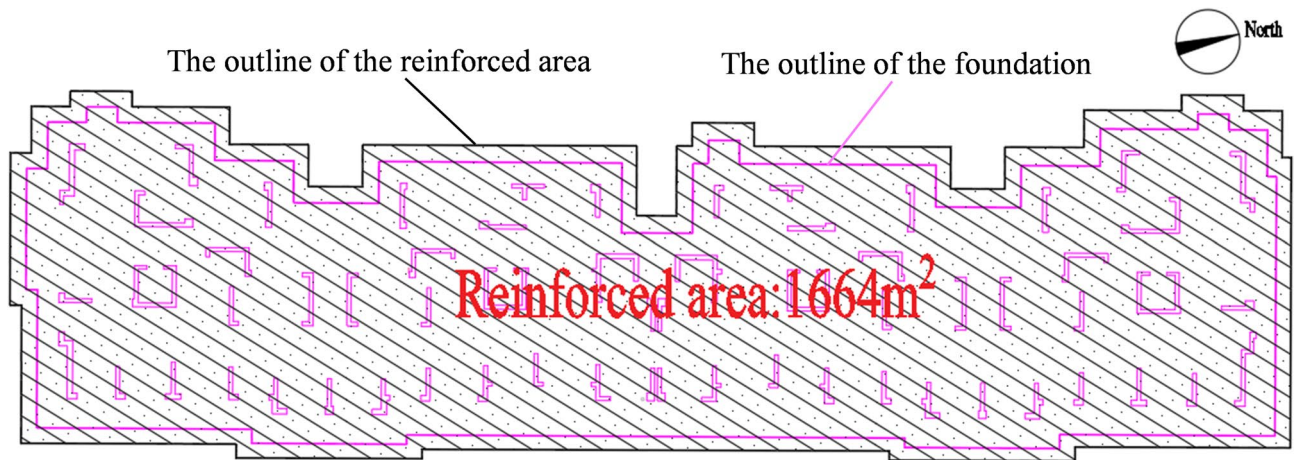


Fig. 17. The range of grouting reinforced area.

Classification	Project	Param
Grouting holes	Aperture	42 mm
	Hole spacing	4.0–5.0 m
	Hole depth	24.3 m
Reinforcement	Grout proportion	Adjust according to the pressure of grouting.
	Grouting pressure	0.3–1.5 MPa
	Slurry condensation speed	10–90 s
	Grouting diffusion radius	≥ 2.5 m
	Grouting rate	$\geq 8\%$

Table 4. Parameters for the grouting uplift technique.

where: $\Delta\varepsilon_V$ represents the volume strain of the soil; V_0 is the original volume of the soil.

A “virtual” expansion pressure is gradually applied to the grouting element until the volume strain of the element reaches the volume strain value of the grouting soil, as shown in Fig. 21. The final selected expansion pressure was 1.2 MPa.

Therefore, during the simulation, the constitutive material is first set up in the stratum cavity to achieve grouting and backfilling of the stratum. Then, the soil in the grouting area is set as the constitutive material for reinforcing the soil, and expansion pressure is applied. According to the construction plan, simulate the grouting uplift from east to west. Finally, the purpose of simulating the grouting correction of buildings is achieved.

Feasibility analysis

Referring to similar numerical studies that adopted the volumetric strain method to simulate the uplift caused by grouting^{6,10} the numerical simulation results of this study are consistent with those studies in terms of the uplift trend and stress redistribution, further verifying the reliability of the results. The numerical simulation results of the building settlement before grouting uplift and the numerical simulation results of the building settlement after grouting uplift are compared as shown in Fig. 22. The practical application of building grouting uplift technology has achieved good results and corrected the uneven settlement of buildings. After the completion of the building grouting uplift, the maximum lifting value of the foundation reaches 160 mm, the maximum settlement of the building is reduced to -83 mm, and the maximum settlement difference is reduced to 36 mm. According to the lifting requirements of the building, the maximum eastward deviation of the top of the building is reduced to less than 33 mm, and the maximum tilt is reduced to 0.41%.

In order to ensure the safety of the floor, the stress calculation results of the building are extracted and analyzed, as shown in Fig. 23. In the process of foundation grouting uplift, the basement soil pressure is transferred to the raft, and then to the upper shear wall and floor. According to the calculation results, except for the partial corner of the wall and the position of the bottom plate, the result is too large due to the singularity of the grid; the other bottom plates are subjected to less stress, and the force meets the requirements. After the completion of grouting uplift, the stress of the building is greatly reduced, and the stress of each structure position is less than the design value of the tensile strength of concrete, which ensures the safety of the structure.

The numerical simulation results show that the deviation correction by grouting can play a good role in correcting the deviation. In the process of grouting, it is necessary to pay attention to the grouting pressure of each grouting hole position in real time, coordinate the lifting value of each grouting hole position, and ensure that the relative settlement interpolation of the building is stable within the acceptable range, otherwise it will

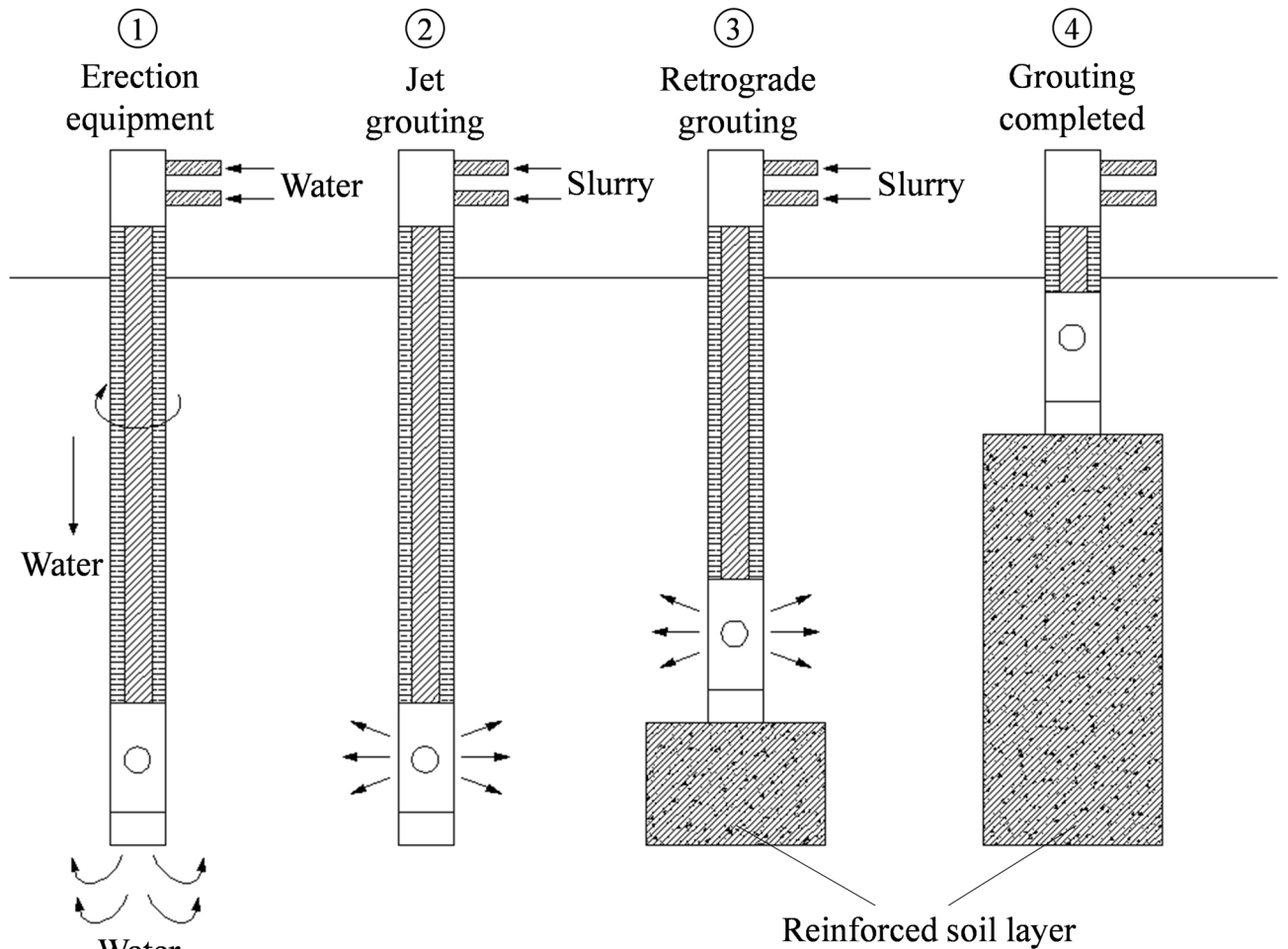


Fig. 18. Schematic diagram of backward grouting.

Number	Construction	Explanation
1	Grouting hole positioning	According to the design requirements for the grouting hole positions, mark the location on the construction site.
2	Drilling rig installation	After the drilling rig is installed, it is leveled, centered, and the angle of the drill rod is adjusted.
3	Drilling rig boring	The drilling diameter is set to 42 mm. Records should be kept during the drilling process to provide reference data for the reinforcement operation.
4	Slurry preparation	The slurry mixture must be screened through a sieve before it can be fed into the machine. The slurry mixing time should not be less than 3 min to prevent the slurry from being mixed unevenly.
5	Grouting construction	Strictly control the injection pressure of each grouting reinforcement hole, and the grouting reinforcement construction must be carried out continuously.
6	Sealing of grouting holes	After grouting reinforcement is completed, the grouting hole is sealed and leveled with a high concentration of the original grout.

Table 5. Grouting construction process.

increase the uneven settlement degree of the building and increase the risk of building tilt. During grouting, the design principle of “first consolidation and then lifting” should be strictly followed to minimize the impact of the lifting process on the original geological conditions and ensure the long-term normal use of the building after grouting uplift.

Evaluation of the building lifting effect Field monitoring program

The grouting uplift construction process is equipped with an automatic monitoring instrument for real-time monitoring. The entire automated monitoring system is composed of multiple monitoring components that work in coordination to jointly achieve the system’s automated monitoring function, as shown in Fig. 24. As

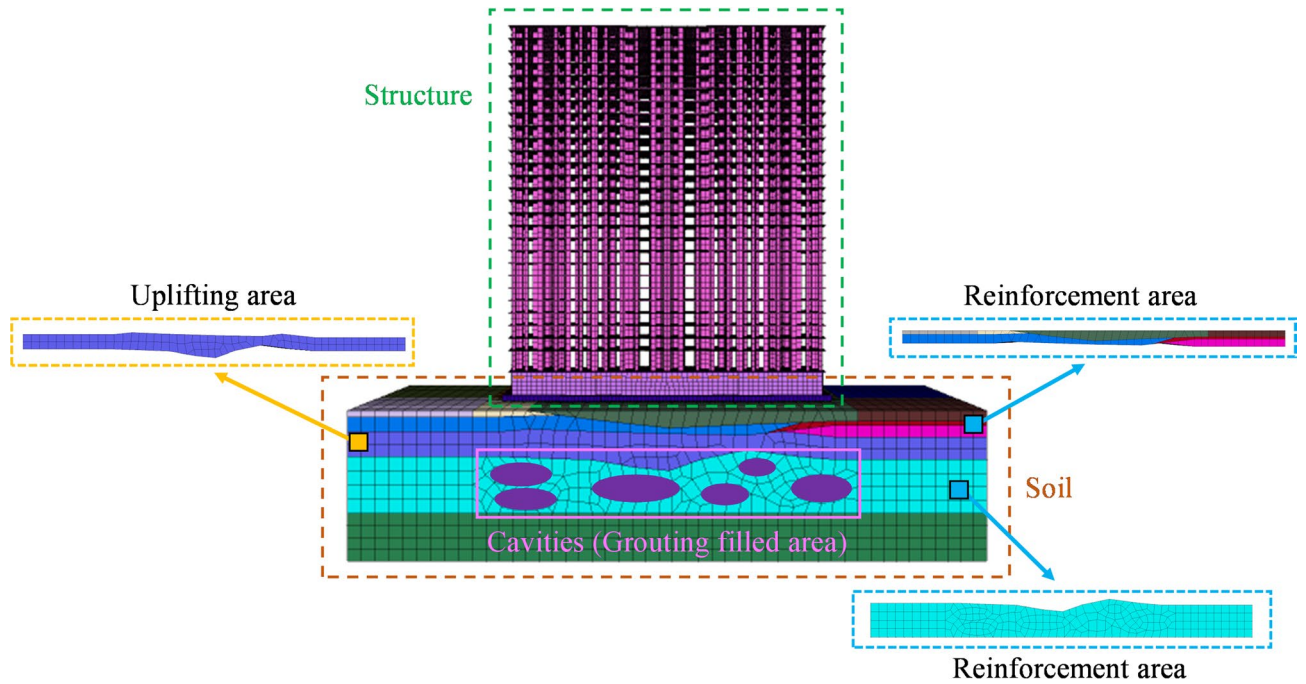


Fig. 19. Schematic diagram of numerical model for grouting uplift.

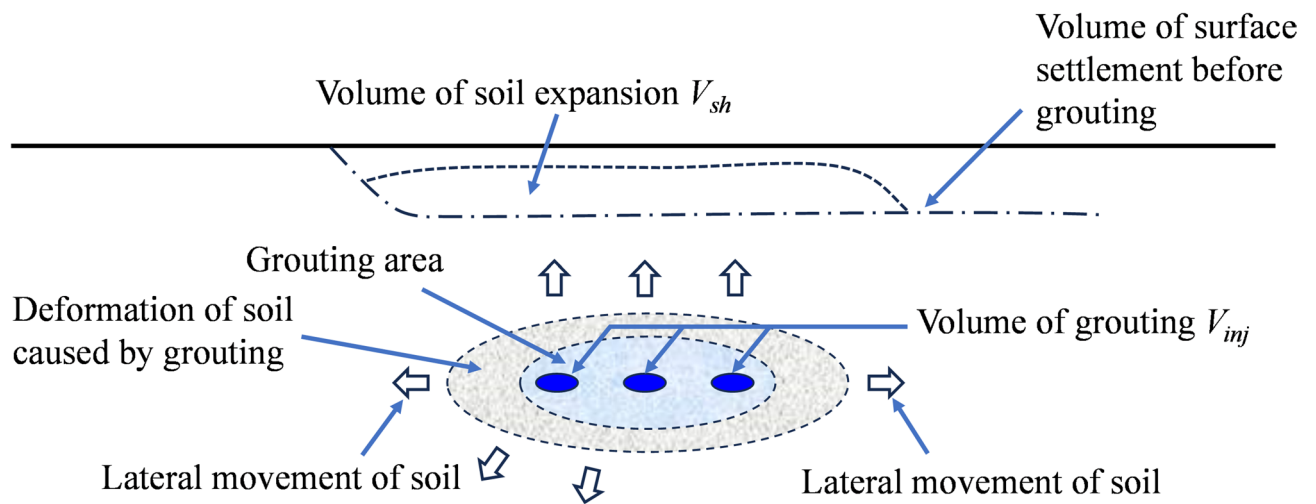


Fig. 20. Schematic diagram of grouting uplift mechanism.

an advanced monitoring technology, automatic monitoring has the characteristics of high precision, strong real-time, high degree of automation, wide application range, etc., but it also has some shortcomings such as limited by satellite signals, high equipment installation and maintenance costs, and difficult data processing and analysis. The automated monitoring system is based on an integrated multi-source sensor architecture. The pressure monitoring module employs a vibrating wire pressure sensor (model GYZ-500 A) with a measurement range of 0–5 MPa and a linear error of $\leq 0.2\%$ Full Scale. Displacement monitoring is achieved using a laser CCD distance meter (Leica DISTO D8), which provides a resolution of 0.01 mm; the system’s overall accuracy has been validated through closed-loop measurements with a total station, ensuring a maximum deviation of ± 1.5 mm within a 50 m range. The data acquisition module integrates a 24-bit Σ - Δ analog-to-digital converter (ADS1256), delivering a theoretical signal-to-noise ratio of 116 dB at a sampling frequency of 1 kHz.

The main monitoring periods are pre-construction measurement, construction monitoring, and post-construction monitoring.

1. Pre-construction measurement: Conduct a settlement measurement before the formal grouting reinforcement construction to record the settlement status.

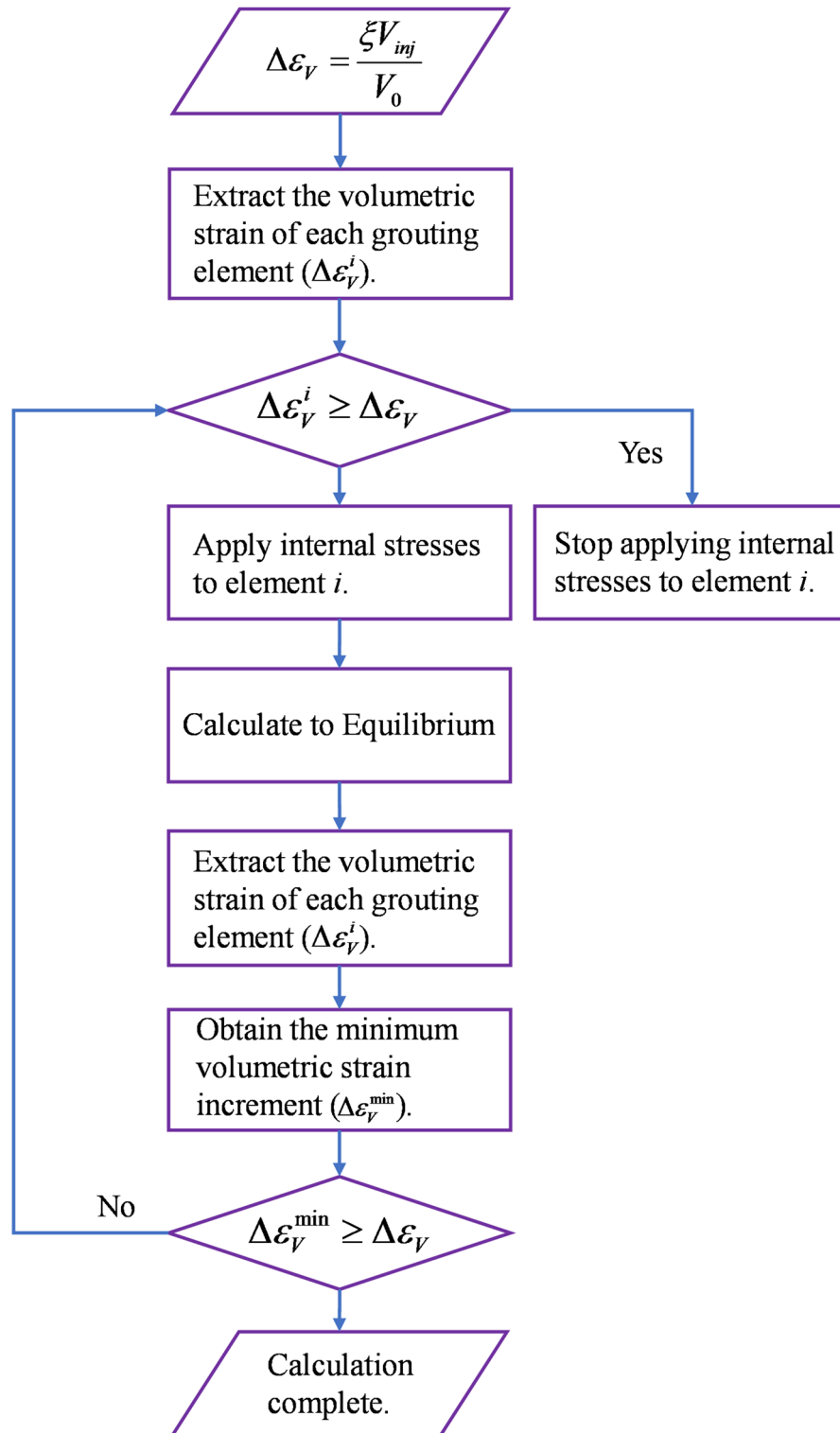


Fig. 21. Flow chart of numerical simulation of grouting.

2. Monitoring during construction: It is necessary to monitor the lift and tilt of the building every day during the construction process to ensure the safety of the building structure.
3. Post-construction monitoring: The settlement monitoring will be carried out three times within one year after the completion and acceptance of the project, and the observation data will be recorded.

The grouting uplift holes are mainly distributed around the building structure, and the automatic monitoring equipment is prone to interference from the surrounding environment, which affects the stability of data

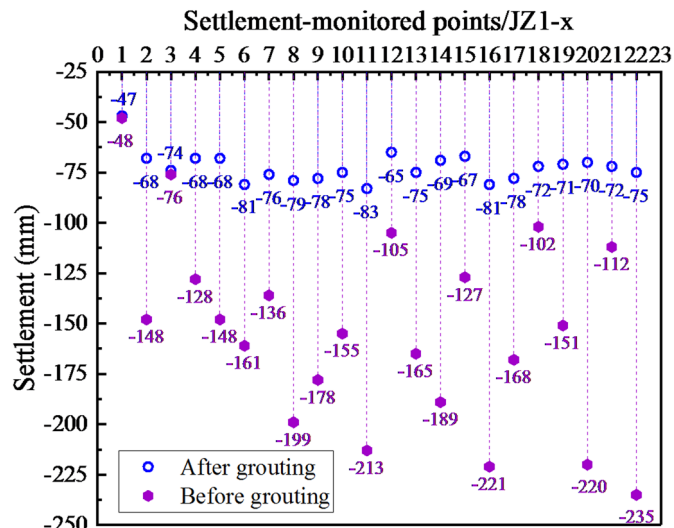


Fig. 22. Comparison of simulation results of building settlement before and after grouting uplift.

transmission, and manual inspection is required to ensure the normal operation of the equipment. Therefore, 20 observation points are temporarily arranged around the building in the area requiring lifting and correction, as shown in Fig. 25.

Analysis and evaluation of monitoring data

Real-time monitoring of the building will be conducted during the construction process, starting from February 25, 2023, and lasting until the completion of the project on April 10, 2023, with a total construction period of approximately 45 days. After the grouting uplift project was completed, the cumulative uplift at the monitoring point is shown in Fig. 26. Figure 26(a) illustrates that the upward displacement of the building varies in degrees. And the upward displacement on the east side is greater than on the west side. The maximum cumulative upward displacement reaches 94.07 mm at monitoring point F7, representing approximately 49% of the total settlement value achieved at this location. Point F4 exhibited the most significant initial settlement. This point has a cumulative upward displacement of 91.55 mm. This displacement represented 42.4% of the total settlement value at this location. In the area where there was previously a small settlement, the corresponding upward displacement is also small. The monitoring results after grouting confirmed that the settlement relief effect was obvious. It can be seen from Fig. 27(b) that after the 10th grouting, the uplift at points F13 to F19 has tended to stabilize. The remaining measurement points began to show obvious bulging after the second grouting and tended to stabilize after the 17th grouting. The figure demonstrates that the lifting trends at all monitoring points align with the grouting construction plan. And the building uplifts successively from east to west.

Figure 27 illustrates the comparison between the structural settlement monitoring values recorded after grouting uplift and those obtained before this intervention. The maximum east-west settlement differential of the building has been reduced to less than 30 mm, while the maximum eastward deviation at the top of the structure is now below 33 mm. Additionally, the maximum tilt has been minimized to 0.41‰, thereby conforming to established acceptance criteria.

The comparison between the field monitoring value and the numerical simulation results of the building settlement after grouting uplift is shown in Fig. 28. The geological conditions are inherently complex, rendering it ambiguous to what extent the actual uplift of the formation correlates with the grouting pressure; furthermore, there exist inherent discrepancies in controlling the grouting pressure at each injection well location. In the numerical simulation, the formation conditions are simplified, and the grouting pressure is uniform, which leads to a large gap between the field monitoring results and the numerical simulation results. Therefore, in the actual grouting uplift construction, it is necessary to conduct a supplementary survey on the formation conditions before the foundation grouting uplift to understand the formation conditions in detail. In the construction process, the complex formation conditions should be timely addressed. The depth of grouting holes should meet the design requirements, the grouting pressure value should be adjusted at any time during the grouting process, and the formation lifting situation should be noted to ensure that the grouting uplift of the building meets the design requirements.

Discussion and outlook

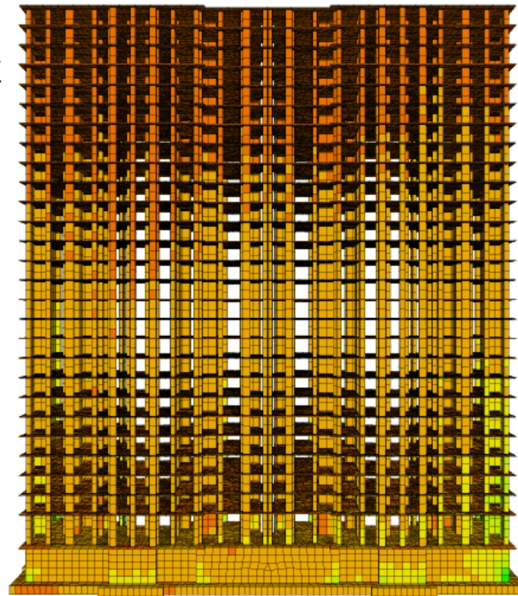
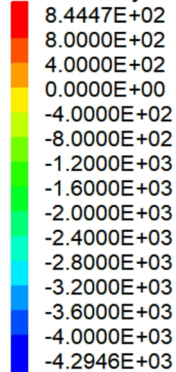
Although the grouting uplift technology for buildings is widely applied and has achieved remarkable results, it has some inherent flaws and limitations. The flow path of the grout in underground fissures, pores, or weak layers is difficult to control precisely. Due to the non-homogeneity of geological conditions, the uncertainty of grout flow, and the limitations of grouting hole layout, it is hard to achieve completely uniform and synchronous lifting of all parts of the building. This may lead to insufficient or excessive lifting in some areas and even cause new tilting or distortion. Uneven lifting or a significant stiffness difference between the slurry stone body and the

FLAC3D 6.00

©2019 Itasca Consulting Group, Inc.

Zone Minimum Principal Stress

Calculated by: Constant



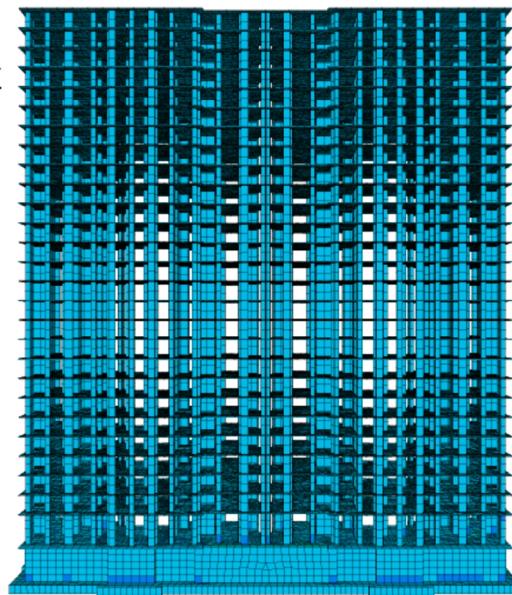
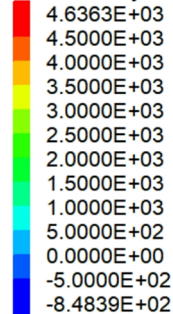
(a)

FLAC3D 6.00

©2019 Itasca Consulting Group, Inc.

Zone Maximum Principal Stress

Calculated by: Constant



(b)

Fig. 23. Calculation result of building stress after grouting uplift. (a) Minimum principal stress, (b) Maximum principal stress.

surrounding soil may cause excessive additional stress on the foundation slab or upper structure components, leading to cracking. Suppose the lifting speed is not properly controlled. In that case, overly rapid lifting may subject the upper structure (especially those already damaged) to excessive dynamic forces or deformations, resulting in new cracks or damage. The lifting process may exert pulling or shearing forces on the connection points between buildings and underground pipelines (such as water pipes, gas pipes, cables, etc.), causing damage. Moreover, during the curing process of cement-based slurry, shrinkage occurs, which may lead to partial settlement of the lifting effect, affecting the stability and durability of the final lifting amount.

This research takes the settlement phenomenon of buildings in Mengshan County, Guangxi as the research background, aiming to attempt to solve some of the existing defects in the grouting uplift technology of existing buildings. The researchers conducted a detailed supplementary geological investigation of the area where the building with uneven settlement was located. Before carrying out the grouting uplift work on the buildings,

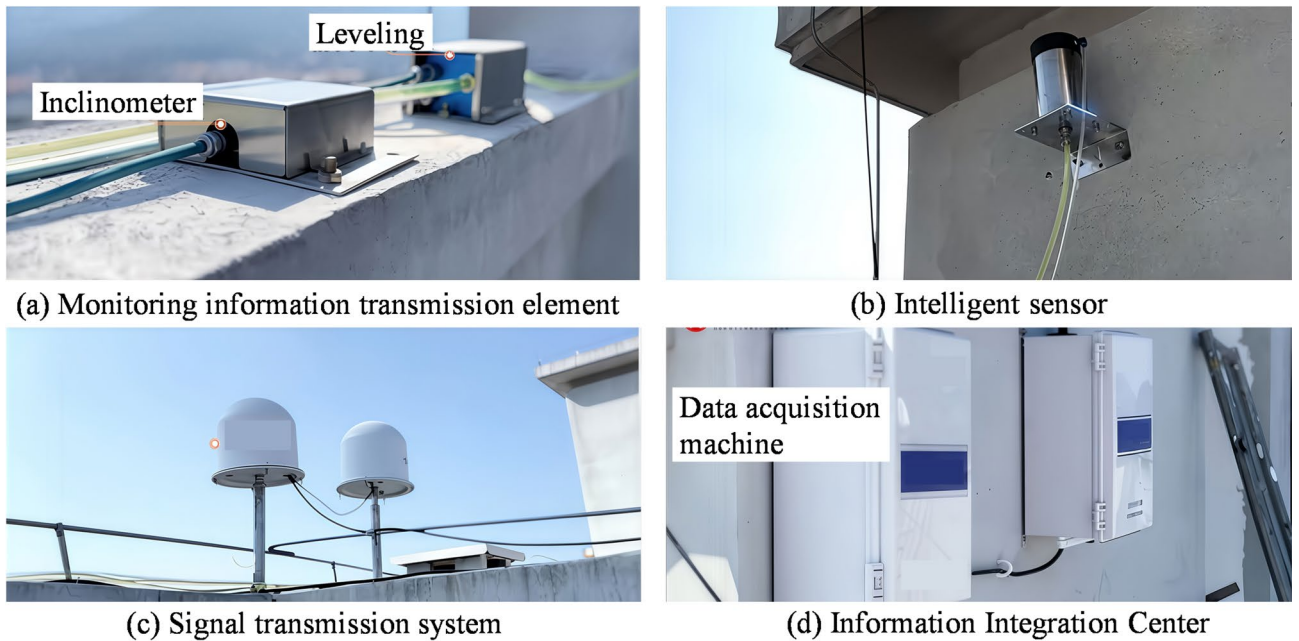


Fig. 24. Schematic diagram of automated monitoring equipment.

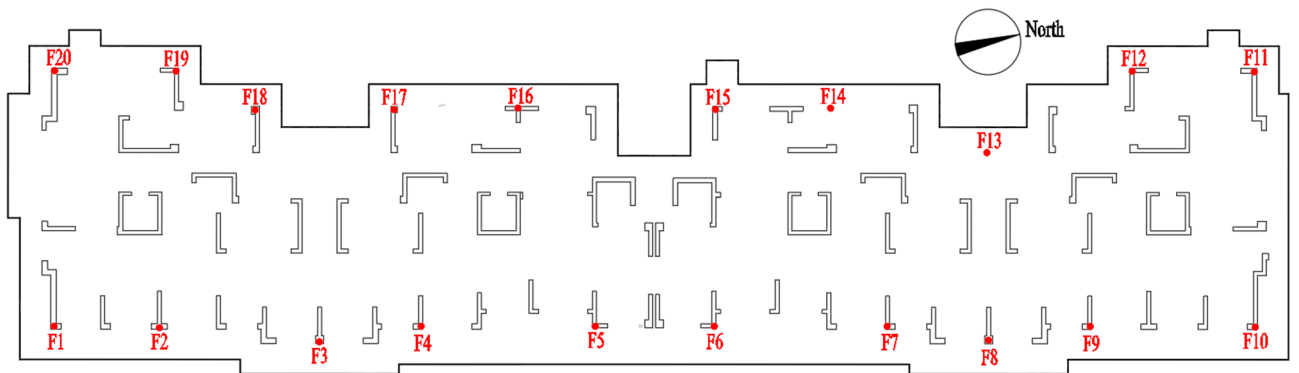
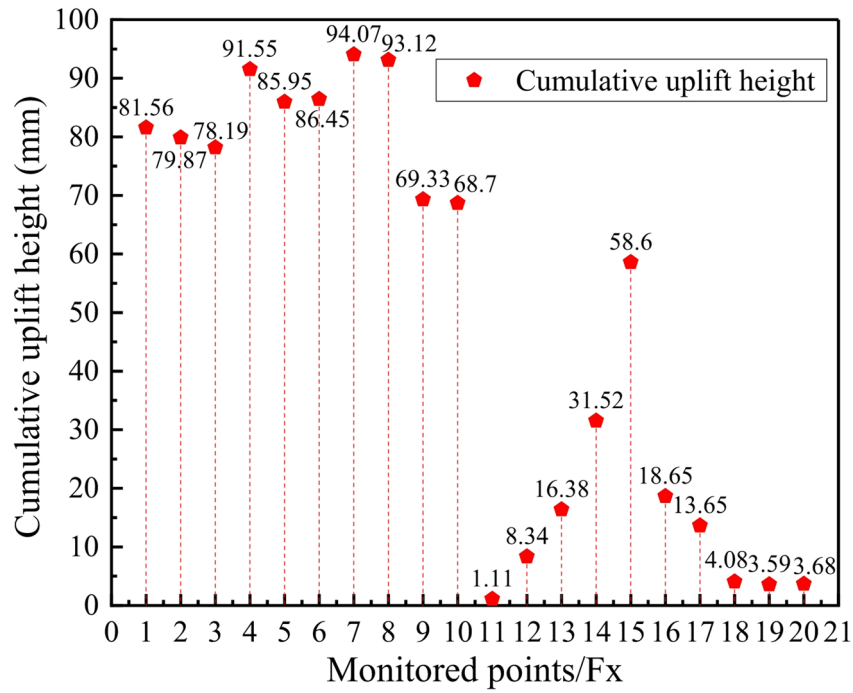


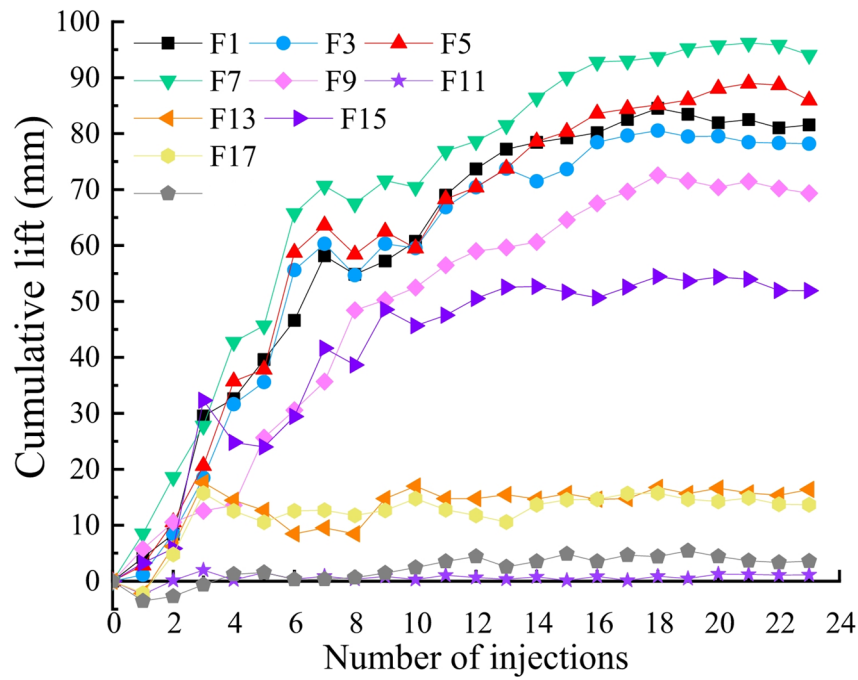
Fig. 25. Schematic diagram of automatic monitoring equipment installation position.

numerical simulation was used to explore the settlement mechanism of the buildings and analyze the feasibility of grouting uplift. Through the analysis of the numerical simulation calculation results, it can be known that the existence of cavities is the main cause of uneven settlement of the building. During the grouting uplift process, corresponding grouting uplift schemes were also designed for the strata containing cavities. Compared with the conventional grouting uplift technology, the grouting uplift technology in this study has the following advantages:

1. High-aluminum iron special composite slurry is selected as the grouting material. The curing time and diffusion range of this slurry are controllable, and it has good permeability. The structure formed after curing has high strength and strong impermeability, and does not shrink after consolidation. This initially solves the problem of uncontrollable curing time and diffusion range of the slurry in the traditional grouting uplift technology, and overcomes the partial settlement of buildings caused by the shrinkage of the slurry after curing.
2. A detailed geological investigation was conducted. Before carrying out the grouting uplift work on the building, the settlement mechanism of the building was explored through numerical simulation, and the feasibility of grouting uplift was analyzed. The stratum beneath the building was strengthened before grouting uplift. Based on the results of numerical simulation analysis, the design of grouting hole positions, depths, and spacings was optimized. This reduced the mutual interference between different grouting holes and maximized the uniform and synchronous lifting of all parts of the building.
3. In response to the problem of uneven settlement of the building caused by underground cavities in the case study that this research is based on, this paper proposes a staged grouting mode of “reinforcement followed



(a)



(b)

Fig. 26. Monitor the lifting situation of the monitoring points. (a) Cumulative uplift of the structure after the completion of grouting uplift., (b) Typical monitoring points' vertical displacement and cumulative uplift change curve.

by uplift". Firstly, the cavities in the strata beneath the building are filled; after the grouting material in the filled cavities has completely solidified and the weak strata have been effectively reinforced, the grouting uplift construction of the upper building is carried out. This approach aims to minimize the disturbance to the deep weak strata during the construction process and ensure that all parts of the building structure can

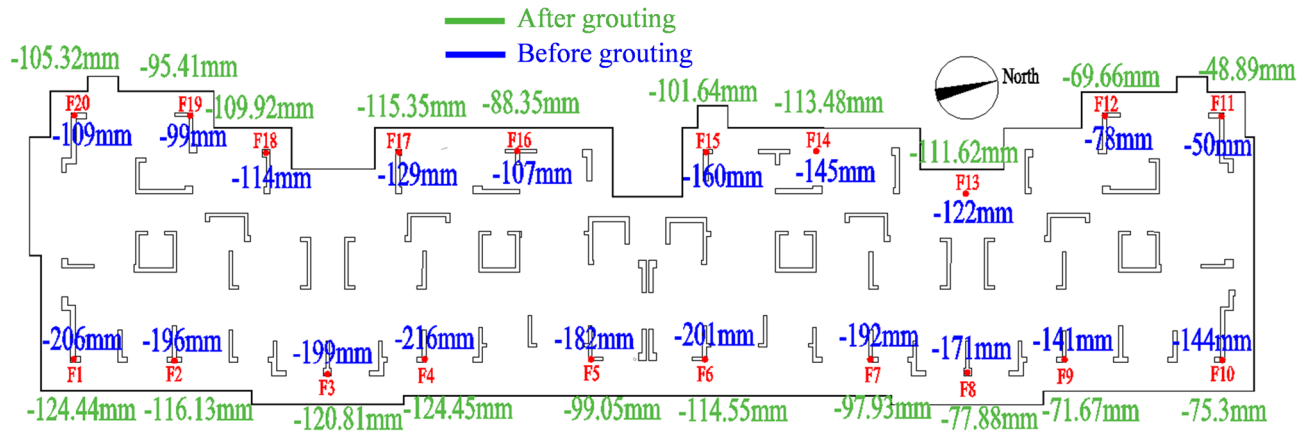


Fig. 27. Comparison of building settlement before and after grouting uplift.

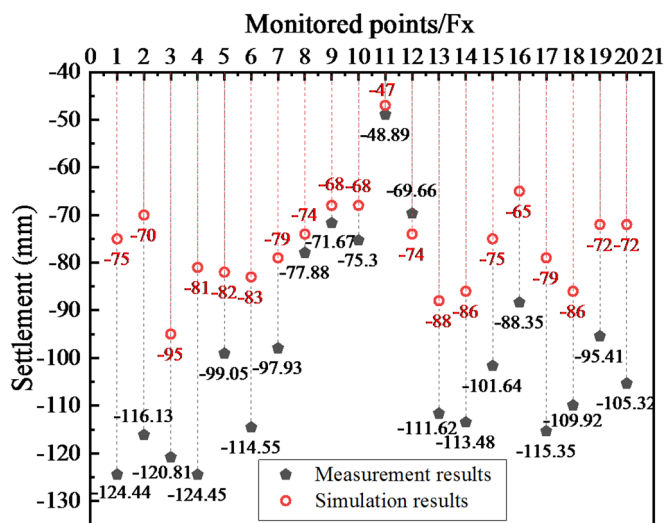


Fig. 28. Comparison of numerical simulation and field monitoring before and after grouting uplift.

be lifted evenly, thereby overcoming the technical limitations of the traditional single-stage grouting uplift technology when dealing with the settlement of buildings in strata with cavities.

4. A strategy of sequential, phased, and slow grouting with low grouting pressure was adopted, strictly controlling the height of grouting lift for each part of the building. During the lifting process, 10 sets of equipment were used simultaneously for continuous operation, lifting from the areas with larger settlement values to those with smaller ones in a cyclic manner. This was done to prevent as much as possible the new tilting, distortion, cracking, or damage to the building caused by insufficient local lifting, excessive local lifting, or improper control of the lifting speed.
5. During the grouting lifting process, an automated monitoring instrument is equipped for real-time monitoring. As an advanced monitoring technology, automated monitoring features high precision, strong real-time performance, a high degree of automation, and a wide application range. The low grouting pressure and slow grouting strategy adopted in this study, in combination with the real-time monitoring system, provide emergency response time for the grouting uplift construction personnel, preventing secondary damage to the building caused by uneven lifting.

The grouting uplift technology for buildings still has many limitations, which require researchers to make joint efforts to improve this technology further.

Conclusion

This study addresses the uneven settlement issue of a high-rise building in Mengshan County, Guangxi, and develops a targeted grouting uplift technology. Through integrated geological investigation, FLAC3D numerical simulation, and field monitoring, the core causes of settlement are clarified, and the effectiveness of the proposed scheme is verified. Key scientific insights and engineering contributions are summarized as follows:

1. High-porosity strata with loose structure and strong permeability are the primary geological drivers of uneven settlement, as they easily form cavities and reduce foundation bearing capacity. Numerical simulation confirms that stratum cavities significantly exacerbate settlement unevenness, providing a critical basis for targeted treatment.
2. A two-stage “reinforcement-first, then uplift” grouting strategy is proposed: filling stratum cavities and reinforcing shallow/deep strata prior to uplift, with the intermediate zone designated as the uplift area. This design ensures uniform building elevation and mitigates risks of secondary deformation.
3. The adopted high-aluminum iron composite slurry resolves key limitations of traditional grouts, featuring controllable setting time (10–90 s), minimal shrinkage (< 0.02%), and adjustable diffusion range (≥ 2.5 m), effectively preventing post-construction re-subsidence.
4. Optimized grouting hole layout combined with phased, low-pressure (0.3–1.5 MPa), and slow grouting minimizes structural damage from improper local lifting. Field application reduced the building’s tilt from 6‰ to 0.3‰, meeting habitation requirements.
5. For complex strata (e.g., clay, sand, karst), detailed geological investigation and slurry flow control are prerequisite for reliable application. A three-phase long-term monitoring plan (high-frequency initial stage, regular medium-term stage, periodic long-term stage with event-triggered mechanisms) is recommended to ensure long-term structural stability.

Data availability

The datasets used and analyzed during the current study are available from the corresponding author upon reasonable request.

Received: 5 November 2024; Accepted: 31 January 2026

Published online: 25 February 2026

References

1. Yin, H. *Research of Treatment for Inclination of Building on Soft Soil Foundation* (China University of Geosciences, 2008).
2. Li, R. *Finite Element Analysis of Broken Column Jacking Correction of Existing Frame Structures* (Hebei University of Architecture, 2024). <https://doi.org/10.27870/d.cnki.ghbjz.2024.000113>
3. Dai, H. *Analysis and Rectification Method of Overall Inclined RC Frame Structure* (Changsha University of Science & Technology, 2023). <https://doi.org/10.26985/d.cnki.gcsjc.2023.001069>Changsha, China.
4. Ministry of Housing and Urban-Rural Development of the People’s Republic of China (MOHURD). *Code for Design of Building Foundation (GB 50007–2011)* (China Architecture & Building, 2011).
5. Li, Y., Zhang, D. & Fang, Q. Study on safety control technology of upper building crossed by shallow metro tunnel. *China Civil Engineering Journal*. 48(S1), 266–269. DOI: CNKI: SUN: TMGC.0.2015-S1-044 (in Chinese). (2015).
6. Ni, J. & Cheng, W. Using fracture grouting to lift structures in clayey sand. *J. Zhejiang Univ-SC A*. 11, 879–886. <https://doi.org/10.1631/jzus.A0900748> (2010).
7. Zhang, D., Huang, Z., Wang, R., Yan, J. & Zhang, J. Grouting-based treatment of tunnel settlement: practice in Shanghai. *Tunn. Undergr. Sp Tech*. 80, 181–196. <https://doi.org/10.1016/j.tust.2018.06.017> (2018).
8. Bai, Y., Yang, Z. & Jiang, Z. Key protection techniques adopted and analysis of influence on adjacent buildings due to the bund tunnel construction. *Tunn. Undergr. Sp Tech*. 41, 24–34. <https://doi.org/10.1016/j.tust.2013.11.005> (2014).
9. Ni, J. & Cheng, W. Monitoring and modeling Grout efficiency of lifting structure in soft clay. *Int. J. Geomech*. 10 (6), 223–229. [https://doi.org/10.1061/\(ASCE\)GM.1943-5622.0000026](https://doi.org/10.1061/(ASCE)GM.1943-5622.0000026) (2010).
10. Zhang, M., Wang, X. & Wu, Y. Numerical evaluation of uplifting effect for upper structure by grouting. *J. Cent. South. Univ*. 19 (2), 553–561. <https://doi.org/10.1007/s11771-012-1039-9> (2012).
11. Schweiger, H. & Kummerer, C. Numerical modelling of settlement compensation by means of fracture grouting. *Soils found*. 44 (1), 71–86. <https://doi.org/10.3208/sandf.44.71> (2004).
12. Jin, Z. et al. Stability analysis for excavation in frictional soils based on upper bound method. *Comput. Geotech*. 165, 105916. <https://doi.org/10.1016/j.compgeo.2023.105916> (2024).
13. Jin, Z. et al. Probabilistic analysis for excavation stability in spatially variable soil based on upper bound method. *Comput. Geotech*. 176, 106769. <https://doi.org/10.1016/j.compgeo.2024.106769> (2024).
14. Tu, S., Li, W., Zhang, C. & Chen, W. Effect of inclined layered soils on face stability in shield tunneling based on limit analysis. *Tunn. Undergr. Sp Tech*. 131, 104773. <https://doi.org/10.1016/j.tust.2022.104773> (2023).
15. Jin, Z., Zhang, C., Li, W. & Pan, Y. An efficient stability analysis method based on upper bound method for excavation reinforced by composite soil nail wall. *Transp. Infrastructure Geotechnol*. 12 (6), 1–33. <https://doi.org/10.1007/s40515-025-00675-9> (2025).
16. Wu, G. et al. Laboratory tests of an eccentrically loaded strip footing above single underlying void. *J. Building Eng*. 111, 113211. <https://doi.org/10.1016/j.job.2025.113211> (2025).
17. Wu, G., Zhao, M., Zhang, R. & Liang, G. Ultimate bearing capacity of eccentrically loaded strip footings above voids in rock masses. *Comput. Geotech*. 128, 103819. <https://doi.org/10.1016/j.compgeo.2020.103819> (2020).
18. Zhuang, H., Li, X., Zhao, K. & Hu, M. Dynamic sub-structure method for longitudinal seismic response of large-diameter shield tunnel through the complex strata. *Tunn. Undergr. Sp Tech*. 163 <https://doi.org/10.1016/j.tust.2025.106680> (2025).
19. Gollegger, J. Numerical and analytical studies of the effects of compensation grouting. *Austria: Graz University of Technology*, (2001).
20. Sagaseta, C. Analysis of undrained soil deformation due to ground loss. *Geotechnique* 37 (3), 301–320. <https://doi.org/10.1680/geot.1987.37.3.301> (1987).
21. Cui, Y., Tan, Z., Zhou, Z., Wu, J. & Wang, J. Preparation and application of low rebound liquid alkali-free accelerator for shotcrete. *Constr. Build. Mater*. 367, 130220. <https://doi.org/10.1016/j.conbuildmat.2022.130220> (2023).
22. Cui, X. A comprehensive study on damage prediction of pile foundations of inclined high rise buildings and the effect of compaction grouting. *Sci. Rep*. 15 (1), 31813. <https://doi.org/10.1038/s41598-025-17290-w> (2025).
23. Zamanian, M. et al. Comparative efficacy of grouting and mixing methods for stabilizing collapsible soils with nano-clay and cement. *Case Stud. Constr. Mater*. 23, e05159. <https://doi.org/10.1016/j.cscm.2025.e05159> (2025).
24. Zhou, Z., Li, Z., Wang, X., Li, H. & Li, G. Investigation and application of ordinary Portland cement-sulfoaluminate cement grouting material in broken stratum with high-temperature water. *Constr. Build. Mater*. 493, 143323. <https://doi.org/10.1016/j.conbuildmat.2025.143323> (2025).
25. Sha, F., Fan, R., Gu, S. & Xi, M. Strengthening effect of sulphoaluminate cementitious grouting material for water-bearing broken rocky stratum. *Constr. Build. Mater*. 368, 130390. (2023). <https://doi.org/10.1016/j.conbuildmat.2023.130390> (2023).

26. Kyaw, K. N. C., Motohashi, T., Sasahara, S. & Inazumi, S. Evaluation of liquefaction resistance in chemically grouted sand using Cyclic triaxial tests. *Results Eng.* **27**, 106875. <https://doi.org/10.1016/j.rineng.2025.106875> (2025).
27. Sathurshan, M. et al. Compressive strength in grouted dry-stack concrete block masonry: experimental and analytical predictions. *Constr. Build. Mater.* **467**, 140411. <https://doi.org/10.1016/j.conbuildmat.2025.140411> (2025).
28. Zhang, Z., Peng, H. & Rao, X. Numerical simulation study of grouting diffusion process in soft soil foundation. *Rock. Soil. Mech.* **32** (S1), 652–655. <https://doi.org/10.16285/j.rsm.2011.s1.097> (2011).
29. Peng, P., Zhang, D. & Sun, Z. Deformation characteristics of surrounding rock and reinforcement param design of weak interlayer tunnels. *Chin. J. Rock Mechan. Eng.* **40** (11), 2260–2272. <https://doi.org/10.13722/j.cnki.jrme.2021.0255> (2021).
30. Zhang, X., Min, B., Wang, Y., & Zhang, C. Effect of rainfall-induced localized argillaceous limestone softening coupled with internal submersion on tunnel linings. *Eng. Fail. Anal.* **186**, 110500. <https://doi.org/10.1016/j.engfailanal.2025.110500> (2025).

Author contributions

Xuedong Cui developed the concept and performed the data analysis and wrote the manuscript.

Declarations

Competing interests

The authors declare no competing interests.

Additional information

Correspondence and requests for materials should be addressed to X.C.

Reprints and permissions information is available at www.nature.com/reprints.

Publisher's note Springer Nature remains neutral with regard to jurisdictional claims in published maps and institutional affiliations.

Open Access This article is licensed under a Creative Commons Attribution-NonCommercial-NoDerivatives 4.0 International License, which permits any non-commercial use, sharing, distribution and reproduction in any medium or format, as long as you give appropriate credit to the original author(s) and the source, provide a link to the Creative Commons licence, and indicate if you modified the licensed material. You do not have permission under this licence to share adapted material derived from this article or parts of it. The images or other third party material in this article are included in the article's Creative Commons licence, unless indicated otherwise in a credit line to the material. If material is not included in the article's Creative Commons licence and your intended use is not permitted by statutory regulation or exceeds the permitted use, you will need to obtain permission directly from the copyright holder. To view a copy of this licence, visit <http://creativecommons.org/licenses/by-nc-nd/4.0/>.

© The Author(s) 2026